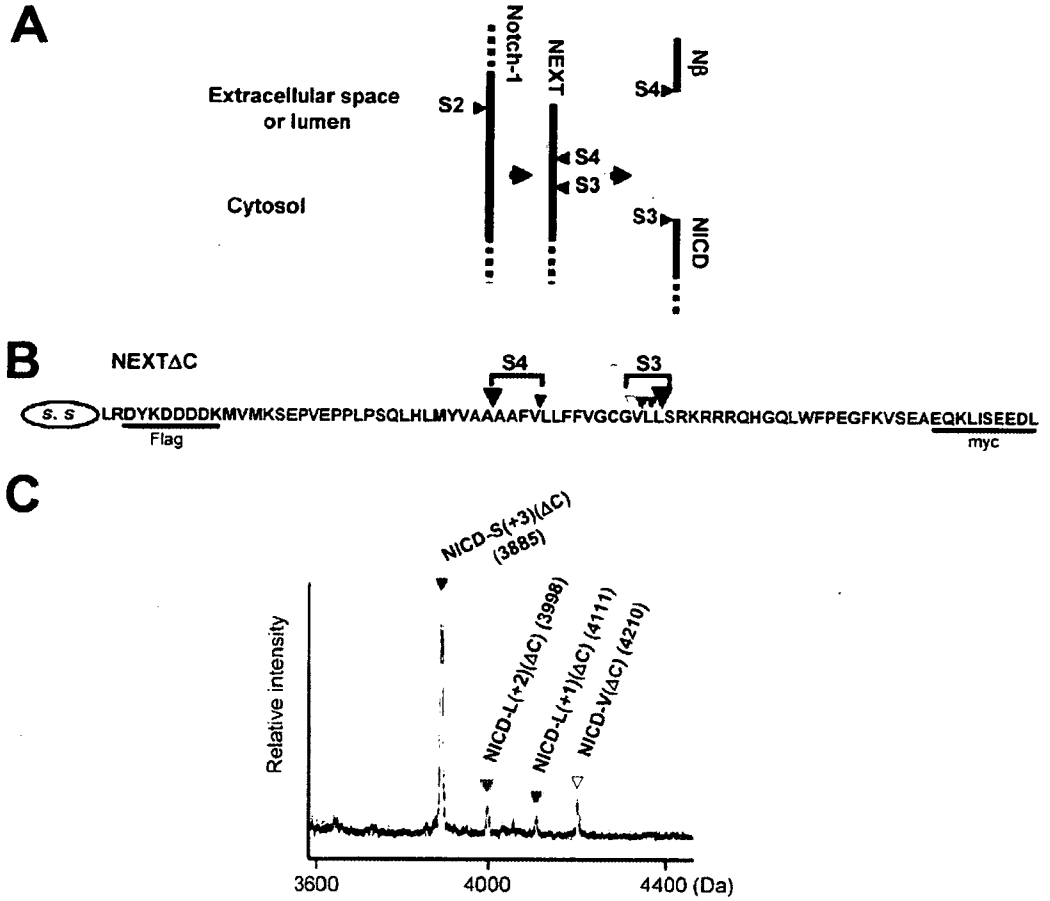

FIG. 1. MALDI-TOF MS analysis of NICD(ΔC) produced by the cell-free Notch-1 cleavage assay. (A) Schematic representation of sequential endoproteolysis of Notch-1. S2 to S4 and the gray area represent the proteolytic sites and the putative TM, respectively. (B) Schematic representation of the NEXTΔC construct used in the cell-free Notch-1 cleavage assay. Colored inverted triangles show the S3 and S4 proteolytic sites. SS, signal sequence. (C) MS spectrum of de novo NICD(ΔC) generated in the cell-free assay. CMF was derived from K293 cells stably expressing NEXTΔC. The molecular mass of each species is indicated. To inhibit degradation by proteases other than aspartyl proteases, BSA and a mixture of metallo-, serine, and cysteine protease inhibitors were added to the cell-free assay buffer. Colored inverted triangles indicate the NICD(ΔC) species produced by cleavage at the sites shown in panel B.

raphy, and immunocytochemistry. The statistical significance of differences was determined by Student's *t* test.

RESULTS

A cell-free Notch-1 cleavage assay indicates diversity in the site of S3 cleavage. The cleavage of the Notch-1 TM occurs at least at two sites, one at S3, which determines the N terminus of intracellularly liberated NICD (39), and the other at S4, which determines the C terminus of extracellularly secreted Nβ (Fig. 1A) (31, 33). We first examined the diversity of the S3 cleavage site. We constructed NEXTΔC, a mouse Notch-1 derivative that lacks the majority of its extracellular and intracellular domains (Fig. 1B), and we established a cell-free Notch-1 cleavage assay using the CMF from cells stably expressing this construct (11). The de novo-generated NICD(ΔC) was immunoprecipitated with anti-myc antibodies and then analyzed by MALDI-TOF MS (Fig. 1C). Strikingly, proteolysis at S3 did not occur at a unique site but rather occurred at multiple sites, as indicated by the presence of multiple sizes of NICD(ΔC) (see Table S1 in the supplemental material). Specifically, proteolysis at S3 occurred at the following sites: S3-L(+1), between Val1744 and Leu1745; S3-L(+2), between Leu1745 and Leu1746; S3-S(+3), between Leu1746 and Ser1747; and the previously reported S3-V, between Gly1743 and Val1744 (39) (Fig. 1B; see Fig. S1A in the supplemental material). Unexpectedly, the highest peak was for NICD-S(+3)(ΔC) rather than NICD-V(ΔC) (Fig. 1C), suggesting that S3-S(+3) is the major site of S3 cleavage under these assay conditions. Addition of the PS/γ-secretase inhibitors eliminated the cleavage at both S3-V and S3-S(+3) (see Fig. S1B in the supplemental material). Moreover, we did not observe generation of these shorter NICD(ΔC) species from the longer NICD(ΔC) (see Fig. S1C in the supplemental material). Therefore, the results are consistent with the possibility that all the fragments are produced by PS-dependent S3 cleavage in the Notch-1 TM.

Diversity in the site of S3 cleavage in living cells. To identify the N terminus of NICD molecules in vivo, we prepared two N-terminal capping antibodies, anti-NT-V (anti-V1744) and anti-NT-S (32), and corresponding recombinant NICD species

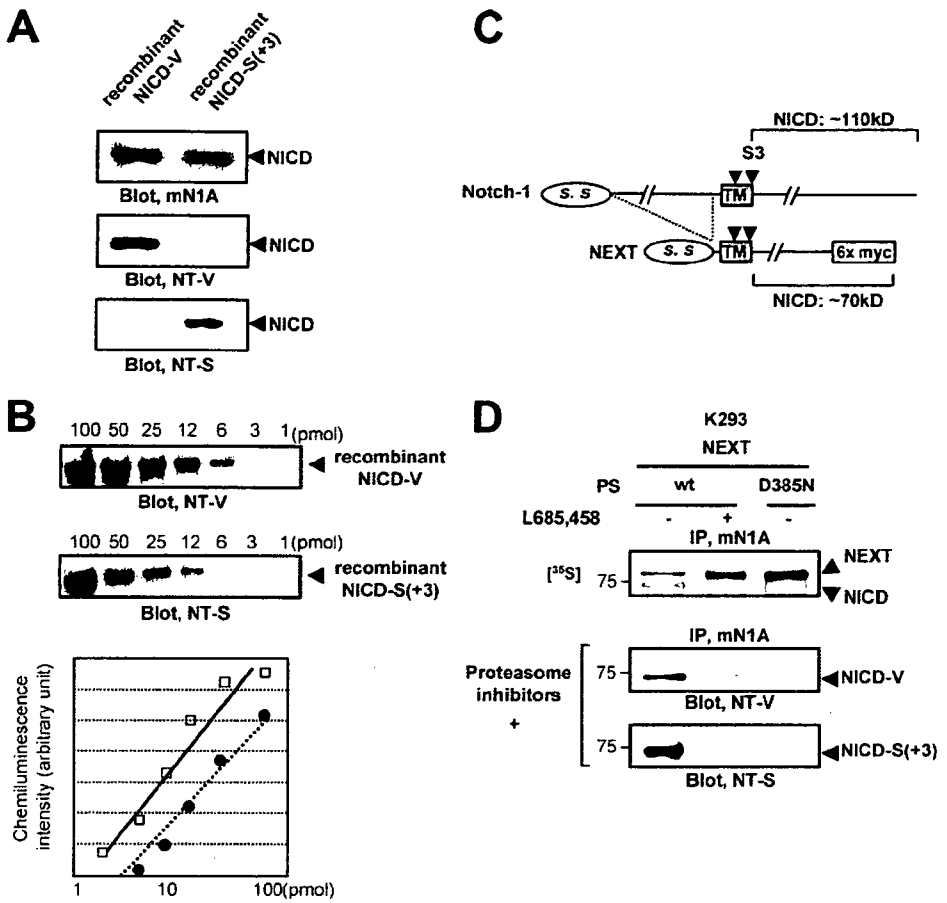

FIG. 2. Characterization of capping antibodies to the N terminus of NICD and detection of distinct NICD species in cultured cells. (A) Specificities of the anti-NT-V and the anti-NT-S antibodies. Immunoblotting with antibody mN1A confirmed that equal amounts of the polypeptides were loaded in each lane (upper panel). (B) Affinities of the anti-NT-V and anti-NT-S antibodies. The indicated amounts of NICD-V or NICD-S(+3) were separated by SDS-PAGE and analyzed by immunoblotting with the anti-NT-V or anti-NT-S antibody, respectively. The graph shows the chemiluminescence intensity versus the concentration of NICD-V (squares) or NICD-S(+3) (circles). Each antibody detected the respective polypeptide in a dose-dependent manner. (C) Schematic representation of Notch-1 and NEXT constructs. The C-terminal portion of the NEXT construct is replaced by myc_6, while full-length Notch-1 has no modification. Note that the molecular mass of NICD generated from NEXT-myc_6 is ~70 kDa, while that of NICD generated from unmodified Notch-1 is ~110 kDa. (D) Generation of NICD-V and NICD-S(+3) in cultured cells. Proteasome inhibitors lactacystin (10 μM), MG262 (100 nM), and NLVS (10 μM) were added to the medium 12 h prior to cell collection.

with distinct N termini (Fig. 2A; see Fig. S2A in the supplemental material). We found that (i) the anti-NT-V antibody specifically recognizes recombinant NICD-V but not NICD-S(+3) (34) (Fig. 2A, middle panel; see Fig. S2B in the supplemental material), whereas the anti-NT-S antibody has the opposite specificity (Fig. 2A; lower panel, see also Fig. S2B in the supplemental material), and (ii) these antibodies can be used to determine the relative amounts of NICD-V and NICD-S(+3) generated, that is, the extents of S3-V and S3-S(+3) cleavage, respectively (Fig. 2B).

Using these capping antibodies, we examined the diversity in the site of S3 cleavage in living cells. The Notch extracellular truncation (NEXT) (Fig. 2C), which lacks the majority of the extracellular domain of Notch-1, undergoes constitutive ligand-independent intramembrane proteolysis by PS/γ-secretase (24). We prepared cells stably expressing NEXT and wt or a dominant-negative form of PS1 (PS1 D385N) (51). A 30-min pulse with [^{35}S]methionine followed by a 2-h chase revealed production of an ~70-kDa NICD band that completely disappeared upon elimination of PS/γ-secretase function (Fig. 2D, upper panel). Because degradation of NICD is mediated by the ubiquitin-proteasome pathway (8, 40, 41), we added a potent proteasome inhibitor mixture consisting of lactacystin, MG262, and NLVS (Fig. 2D, middle and lower panels). The resulting cell lysates were immunoprecipitated with antibody mN1A, separated by SDS-PAGE, and analyzed by immunoblotting with anti-NT-V or anti-NT-S. The anti-NT-V and anti-NT-S antibodies specifically detected the PS-dependent production of NICD-V and NICD-S(+3), respectively (Fig. 2D, middle and lower panels; see Fig. S2C in the supplemental material). We also confirmed that both NICD-V and NICD-S(+3) are produced in cells in the absence of the proteasome inhibitor mixture (see Fig. S2D in the supplemental material).

S3 cleavage during Notch signaling produces distinct molecular species of NICD. Because ligand-induced degradation of Notch receptors is initiated at the plasma membrane (PM),

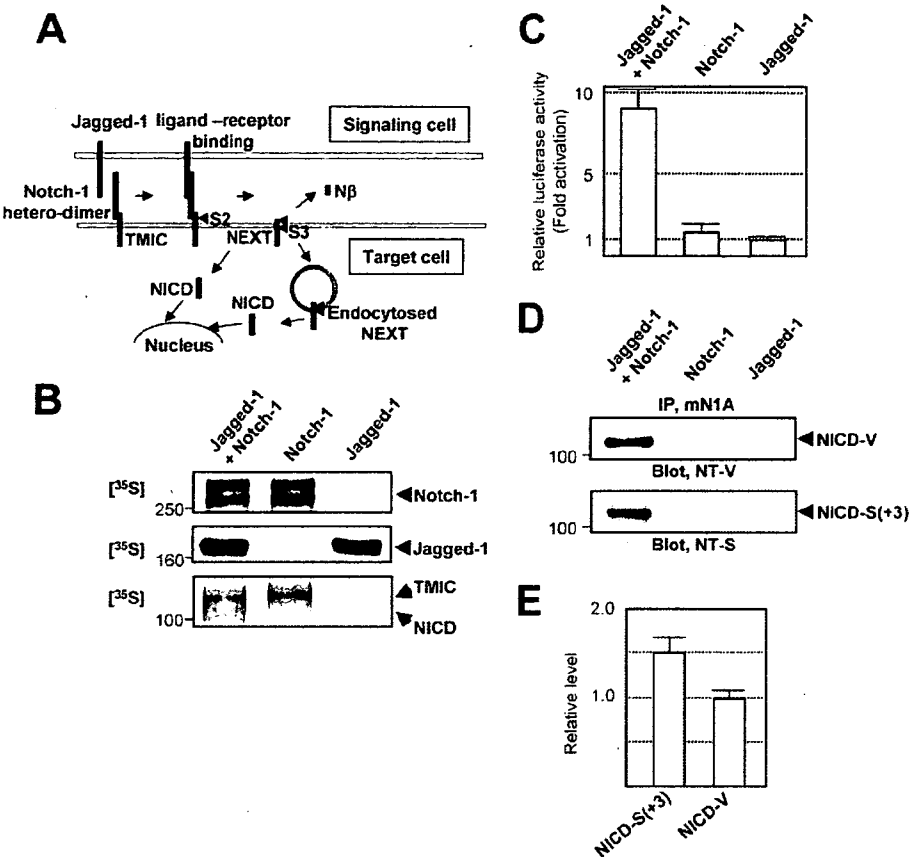

FIG. 3. Detection of different NICD species during Notch signaling. (A) Schematic representation of Notch signaling. (B) Notch signaling in cell culture. CHO(r) cells stably expressing Jagged-1 or Notch-1 were used. Expression of Notch-1 (top panel) and Jagged-1 (middle panel) was determined by a 1-h pulse experiment, followed by immunoprecipitation using antibodies mN1A and H114, respectively. The precipitated proteins were analyzed by SDS-PAGE, followed by autoradiography. A 1-h pulse/2-h chase experiment detected an ~110-kDa NICD band only when the cells were cocultured (bottom panel). (C) Notch signaling was measured using a dual luciferase assay. The relative luciferase activity of Jagged-expressing cells was defined as 1.0. Values represent means ± standard deviations (n = 3). (D) In the presence of the proteasome inhibitors, both NICD-V (upper panel) and NICD-S(+3) (lower panel) were detected during Notch signaling. The bands were detected as described for Fig. 2D. (E) Relative levels of NICD-S(+3) and NICD-V generated during Notch signaling. The relative levels were calculated based on the standard curve shown in Fig. 2B.

intramembrane proteolysis of Notch-1 is thought to occur at restricted subcellular locations, such as the PM and endocytosed vesicles (13, 17, 20) (Fig. 3A). We prepared cells stably expressing either Jagged-1 (a Notch ligand) or full-length Notch-1 and then cocultured them. We determined the extent of Notch signaling using a luciferase reporter assay in cells expressing a newly improved construct, *HES-Y* (see Materials and Methods for details). Pulse-chase experiments revealed that upon coculture, sequential endoproteolysis of Notch-1 occurs, producing the NICD band (Fig. 3B, bottom panel). Moreover, when the cells were cocultured, we observed concomitant activation of the *HES-1* promoter (Fig. 3C). The results therefore demonstrate Notch-1 signaling in cell culture. Using this assay system, we investigated whether NICD-S(+3) and NICD-V are indeed generated during Notch signaling. Strikingly, upon coculture, both NICD-V and NICD-S(+3) were detected (Fig. 3D, upper and lower panels). The intensities of the bands indicated that 1.5-fold more NICD-S(+3) than NICD-V was produced (Fig. 3E). Therefore, the results indicated that there are multiple forms of NICD produced during Notch signaling.

We next tried to detect the NICD-V and NICD-S(+3) in fetal (embryonic day 12, whole embryo without internal organs) and adult (brain) mouse tissues (Fig. 4). Nuclear extracts from these tissues were immunoprecipitated with mN1A, which specifically recognizes intracellular domain of Notch-1 but not Notch-2, -3, or -4. The precipitated proteins were then analyzed by SDS-PAGE, followed by immunoblotting with anti-NT-V or anti-NT-S antibodies. As shown in Fig. 4A, we clearly found both NICD-V (upper panel) and NICD-S(+3) species (lower panel) in the fetal mouse tissues, but these species were barely detectable in adult brains. This is consistent with the finding of a high level of Notch signaling in fetal mouse tissue (22). Moreover, we successfully detected the same NICD-V and NICD-S bands in the mouse embryo even when the combination of antibodies used for immunoprecipitation and immunoblotting was swapped (Fig. 4B). Therefore, the results indicated that multiple forms of NICD are produced in vivo.

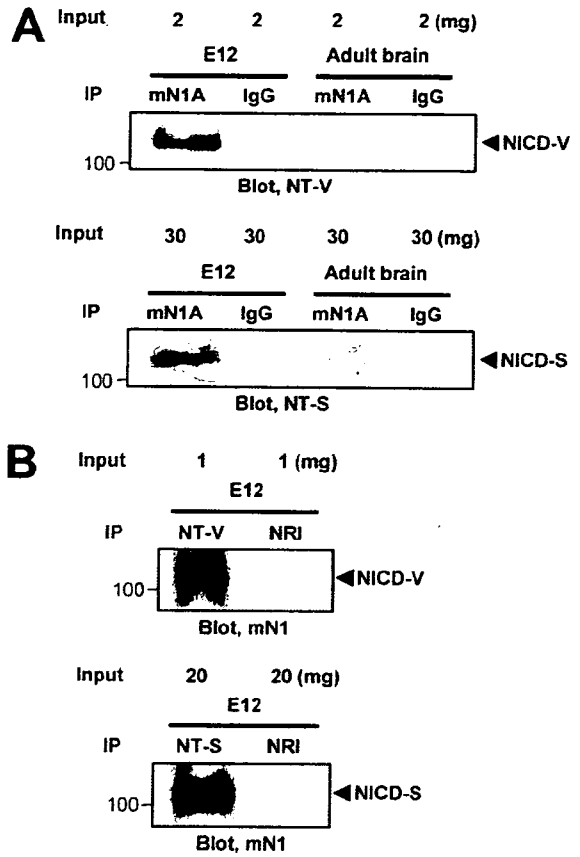

FIG. 4. Detection of NICD-V and NICD-S(+3) in vivo. The indicated amounts of nuclear extracts were loaded for immunoprecipitation. IgG and NRI, isotype-matched immunoglobulin and normal rabbit immunoglobulin, respectively.

Transactivation of the HES-1 promoter by NICD-S(+3) is much weaker than transactivation by NICD-V in living cells. The stability of polypeptides degraded by the ubiquitin-proteasome pathway depends on the N-end rule, where an N-terminal valine is a stabilizing residue and an N-terminal serine is destabilizing (2, 12). Therefore, we examined whether the intensity of Notch signaling differs for NICD-V and NICD-S(+3) in living cells. We loaded *HES-Y*-transfected cells with equal amounts of purified NICD-V or NICD-S(+3) (see Fig. S3 in the supplemental material). After a 1-h loading period, the cells contained similar levels of each NICD species (Fig. 5A). Induction of Notch signaling by chasing the loaded cells for 4 h (signaling period) resulted in much less luciferase activity in the NICD-S-loaded cells than in NICD-V-loaded cells, demonstrating that NICD-S(+3) is much weaker than NICD-V at activating the promoter in living cells (Fig. 5B, left panel).

We next investigated whether the rates of degradation by the proteasome pathway differ for the various species of NICD in an in vitro assay. We incubated recombinant NICD-V or NICD-S(+3) (34) with rabbit reticulocyte lysate (Promega) (12) and examined the levels of the two types of NICD by immunoblotting (Fig. 5C). Our results indicated that NICD-S(+3) is much less stable than NICD-V (Fig. 5D). Moreover, following the proteasome inhibitor treatment, the relative luciferase activities in NICD-S- and NICD-V-loaded cells turned out to be almost the same (Fig. 5E). Collectively the results suggest that unstable NICD-S(+3) may have a much weaker ability than stable NICD-V to mediate intracellular signaling.

The precision of S3 cleavage is distinct in the subcellular locations where it occurs. A previous study showed that the precision of ε cleavage of βAPP, which topologically corresponds to S3 cleavage of Notch-1, differs before and after endocytosis (11). To determine whether S3 cleavage precision differs on PM and endosomes, we performed the cell-free assay using organelles separated by iodixanol gradient fractionation from NEXTΔC-expressing HeLa cells (11). Fractions from a 2.5% to 25% linear iodixanol gradient were examined by immunoblotting with antibodies to early endosome antigen 1 (endosome marker), Na-K ATPase (PM marker), GM130 (Golgi marker), or nicastrin (a component of the PS complex) (Fig. 6A). NICD(ΔC) was generated in the cell-free assay using membranes collected by centrifugation from the endosome-rich (fraction 3) and the PM-rich (fraction 7) fractions and analyzed by immunoprecipitation/MALDI-TOF MS. Remarkably, the relative ratio of NICD-V(ΔC) to NICD-S(+3)(ΔC) was much higher in the PM-rich fraction than in the endosome-rich fraction (Fig. 6B). This indicates that cleavage at S3-V, which generates the longer NICD-V(ΔC), and at S3-S(+3), which generates the shorter NICD-S(+3)(ΔC), occurs predominantly on the PM and endosomes, respectively. This is very similar to the case of ε cleavage of βAPP (11). Subsequently, we investigated the effect of endocytosis on the precision of S3 cleavage. To down-regulate endocytosis, we used cells that express a dominant-negative mutant of dynamin-1 (Dyn-1 K44A) upon tetracycline withdrawal (Fig. 6C) or treatment with bafilomycin A1 (11) (see Fig. S4 in the supplemental material). When endocytosis was strongly inhibited, the precision of S3 cleavage changed drastically, so that the S3-V site instead of the S3-S(+3) site became the major site of cleavage in the cell-free assay (Fig. 6C; see Fig. S4A in the supplemental material). These results from the cell-free assay suggest that generation of stable NICD-V and unstable NICD-S occur predominantly on the PM and endosomes, respectively.

The precision of S3 cleavage changes in parallel with the rate of endocytosis in target cells. Next, we investigated whether these phenomena also occur in living cells. We examined the influence of the rate of endocytosis of NEXT by altering the expression of Dyn-1 K44A in living cells (Fig. 7A). Measurement of biotinylated transferrin uptake revealed various rates of endocytosis in Dyn-1 K44A-expressing cells (Fig. 7B). Strikingly, we found that the ratio of S3-V to S3-S(+3) is low in cells with a high rate of endocytosis and, conversely, that the ratio is high in cells with a low rate of endocytosis (Fig. 7C), which is consistent with the result from the cell-free assay (Fig. 6C). We observed a similar change in the S3 cleavage when endocytosis was blocked with bafilomycin A1 (see Fig. S4B in the supplemental material). Therefore, it appears that the precision of S3 cleavage changes in parallel with the rate of endocytosis, and relative generation of stable NICD-V increases as the rate of endocytosis decreases.

Because Notch signaling is associated with endocytosis of Notch receptors and/or Notch ligands during development (3, 28, 35, 40, 43), we next examined the effect of the change in S3

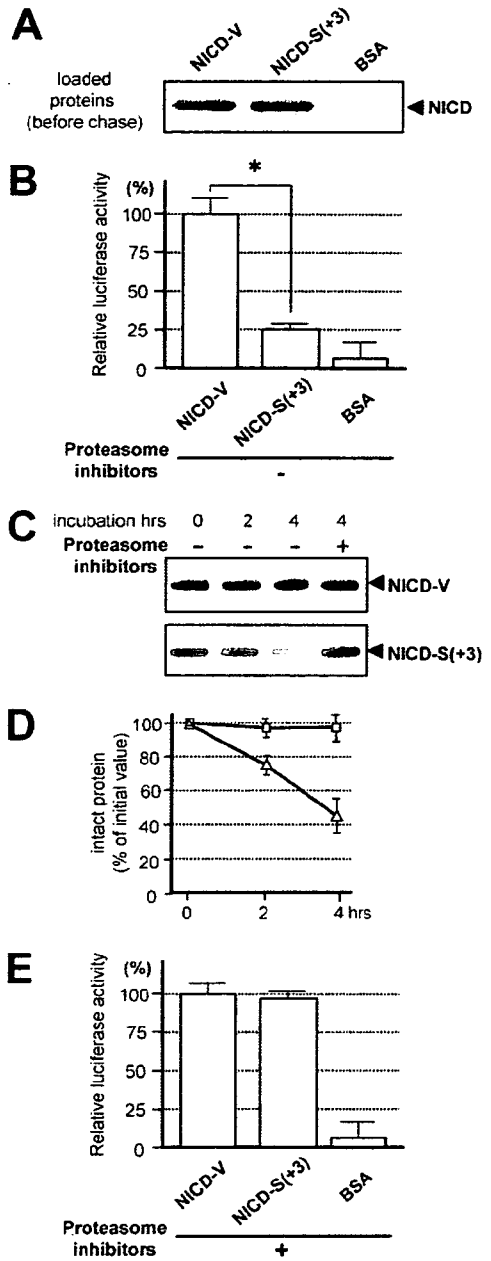

FIG. 5. Characterization of the NICD species. (A) Loading of cells with NICD. HeLa cells (2.5×10^5) were loaded with 5 μg of purified NICD-V, NICD-S(+3), or BSA (control). The cells were collected 1 h after the addition of the Chariot macromolecule complex (defined as the loading period). (B) Assay of Notch downstream signaling induced by the NICD species. The NICD-loaded cells from panel A were chased for 4 h and collected, and Notch downstream signaling was assayed. The values were corrected for background luciferase activity (0.5 μg of β-galactosidase-loaded cells), and the luciferase activity in the NICD-V-loaded cells was defined as 100%. Values represent means ± standard deviations ($n = 3$). The asterisk indicates that the relative luciferase activity in NICD-V-loaded cells is statistically different than that in NICD-S(+3)-loaded cells ($P < 0.001$). Similar results were obtained using cells expressing pGa981-6 (data not shown). (C) Stability of recombinant NICD species in rabbit reticulocyte lysate. Note that the degradation of NICD-S(+3) was inhibited in the presence of proteasome inhibitors. (D) Levels of intact NICDs in the lysates during in vitro degradation. The amount of intact polypeptide was determined using a standard curve of the chemiluminescence intensities of the bands versus their concentrations (data not shown). Squares and triangles indicate the means for NICD-V and NICD-S(+3), respectively. Values represent means ± standard deviations ($n = 3$). (E) Assay of Notch downstream signaling induced by the NICD species in the presence of the proteasome inhibitor mixture. Experiments were performed as described for panel B in the presence of the proteasome inhibitor mixture. The values were corrected for background luciferase activity (0.5 μg of β-galactosidase-loaded cells), and the luciferase activity in the NICD-V-loaded cells was defined as 100%. Values represent means ± standard deviations ($n = 3$).

precision on the intensity of Notch signaling. Surprisingly, we observed a higher intensity of Notch signaling in cells in which the rate of endocytosis of NEXT was lower (Fig. 7D; see Fig. S4C in the supplemental material). These results suggest that the rate of endocytosis in target cells could affect the intensity of intracellular Notch signaling by changing the precision of S3 cleavage and thus its stability.

Mutations around S3 can induce changes in the precision of the cleavage. S3 mutations, such as the Val→Gly mutation (V1744G mutant) and the Lys→Arg mutation (K1749R mutant), cause a decrease in the NICD level (13, 15). To date, this reduction has been considered to be due to decreased NICD generation. However, since we revealed that multiple NICD species with different stabilities are generated, we investigated whether these mutants also change the S3 cleavage precision, which would accelerate degradation of NICD. First, we determined the precision of the S3 cleavage of the Val→Gly mutant version of NEXTΔC in the cell-free assay (Fig. 1C). Strikingly, this mutant was degraded mainly into NICD-L(+1)(ΔC), which has Leu1745 (murine Notch-1 numbering) at its N terminus (Fig. 8A). Therefore, it appears that the Val→Gly mutation causes not only a complete loss of stable NICD-V, but also a dramatic shift in the major product from NICD-S(+3) to NICD-L(+1). We next examined whether NICD-L(+1) behaved like NICD-S(+3) in cellular signal transduction. Like NICD-S(+3), NICD-L(+1) was much weaker than NICD-V at inducing promoter activation in living cells (Fig. 8B). Moreover, our in vitro degradation assay revealed that NICD-L(+1) was much less stable than NICD-V (Fig. 8C). Thus, our in vitro experiments suggested that NICD-L(+1) and NICD-S(+3) are both unstable and have similar effects on Notch signaling but that their effects are distinct from those of NICD-V. We further investigated whether the precision change in the mutant is also observed in living cells. To specifically detect NICD-L(+1), we generated anti-NT-L, an N-terminal capping antibody (see Fig. S5 in the supplemental material). As is clearly shown in Fig. 8D, although almost no NICD-V was detected, a substantial amount of NICD-L(+1) was detected in the Val→Gly version of NEXT-expressing cells. These results indicate that the relative production of unstable NICDs with respect to stable NICD increases in the mutant NEXT cells due to change of the S3 cleavage precision.

The Lys→Arg mutant NEXT (the K1749R mutant) is neither monoubiquitinated nor endocytosed (13). This mutant, like the Val→Gly mutant, causes decreased NICD levels in cell culture (13). Analysis to determine the precision of the S3 cleavage of the Lys→Arg mutant version of NEXTΔC was performed in the cell-free assay. Surprisingly, the Lys→Arg

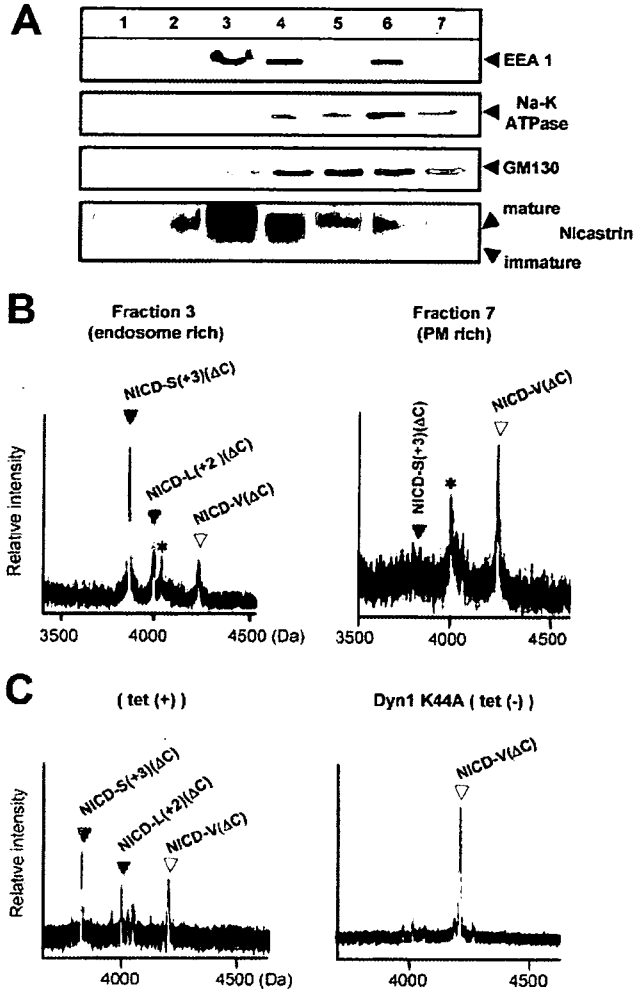

FIG. 6. Subcellular locations where S3-V and S3-S(+3) cleavages occur. (A) Fractions from a 2.5% to 25% linear iodixanol gradient examined by immunoblotting with the indicated antibodies. (B) MS spectra of NICD(ΔC) generated in the cell-free assay using membranes collected by centrifugation from the endosome-rich (fraction 3) and the PM-rich (fraction 7) fractions. Asterisks indicate nonspecific peaks. (C) MS spectra of NICD(ΔC) generated in the cell-free assay. CMFs from HeLa cells stably expressing NEXT(ΔC) and conditionally expressing Dyn-1 K44A were used. The precision of PS-dependent cleavage at the TM-cytoplasmic border in HeLa (left panel) and K293 (Fig. 1C) cells was different, in agreement with a previous report (11).

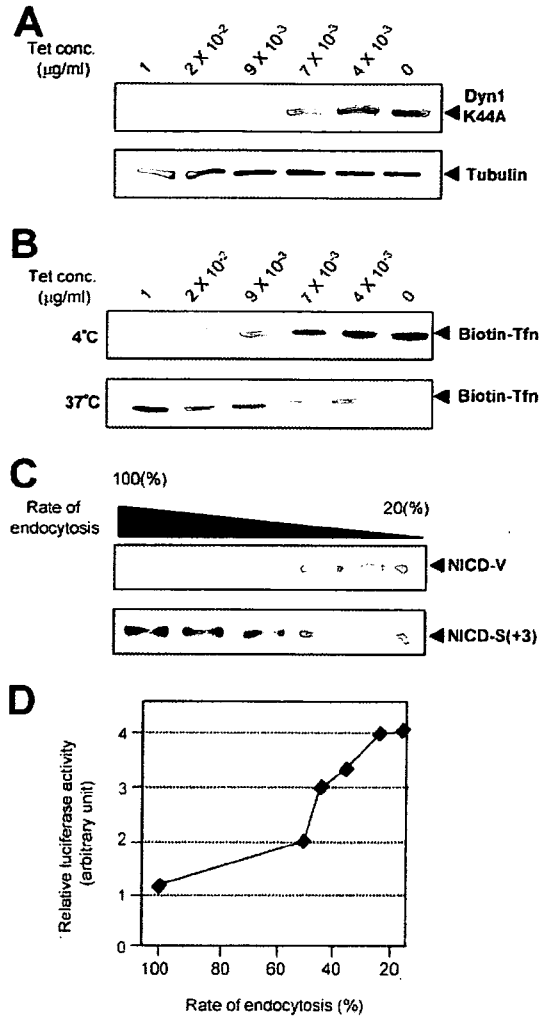

FIG. 7. Parallel change in the rate of endocytosis and the precision of S3 cleavage. (A) Expression of Dyn-1 K44A at various concentrations of tetracycline. Dyn-1 K44A/NEXT-coexpressing HeLa cells were cultured in medium with the indicated concentrations of tetracycline, and cell lysates were examined by immunoblotting with antibody 12CA5 (upper panel) or antitubulin (lower panel). The levels of Dyn-1 K44A increase as the concentration of tetracycline is decreased. (B) Various rates of endocytosis in Dyn-1 K44A expressing cells. Transferrin (Tfn) uptake assays were performed to measure the rate of endocytosis. The ratio of internalized Tfn (37°C; lower panel) to surface-bound Tfn (4°C; upper panel) in cells cultured in medium containing 1 μg/ml of tetracycline was defined as 100%. The rate of endocytosis decreased to ~15% when tetracycline was completely withdrawn. (C) Effect of the rate of endocytosis on the NICD species. The calculated rates of endocytosis were 100%, 41%, 37%, 21%, and 15% in lanes 1 to 5, respectively. (D) A plot of the relative Notch downstream luciferase activity versus the rate of endocytosis at various tetracycline concentrations.

mutant was found to be degraded mainly into NICD-L(+2)(ΔC), NICD-S(+3)(ΔC), and NICD-R(+5)(ΔC) species, which have unstable Leu1746, Ser1747, and the mutated Arg1749 at the N terminus, respectively (Fig. 8E). These results suggest that due to a dramatic change in the S3 cleavage precision, the Lys→Arg mutation causes not only a decrease of NICD-V but also an increase of extra unstable NICD species besides NICD-S(+3). This finding is reminiscent of the S3 cleavage for the Val→Gly mutant NEXT. Moreover, we studied whether NICDs in living cells expressing the Lys→Arg mutant are composed mainly of unstable NICD species. Strikingly, in the cells stably expressing the mutant NEXT, the stable NICD-V was barely detectable (13), while substantial amounts of NICDs were generated in the presence of the proteasome inhibitor mixture (Fig. 8F, top and middle panels). Since almost no NICD is observed in the mutant cells without the inhibitor mixture, it is indicated that NICDs in the Lys→Arg mutant-expressing cells are composed of unstable species (Fig. 8F, bottom panel). Therefore, the changes in the S3 cleavage precision induced by these S3 mutations are at

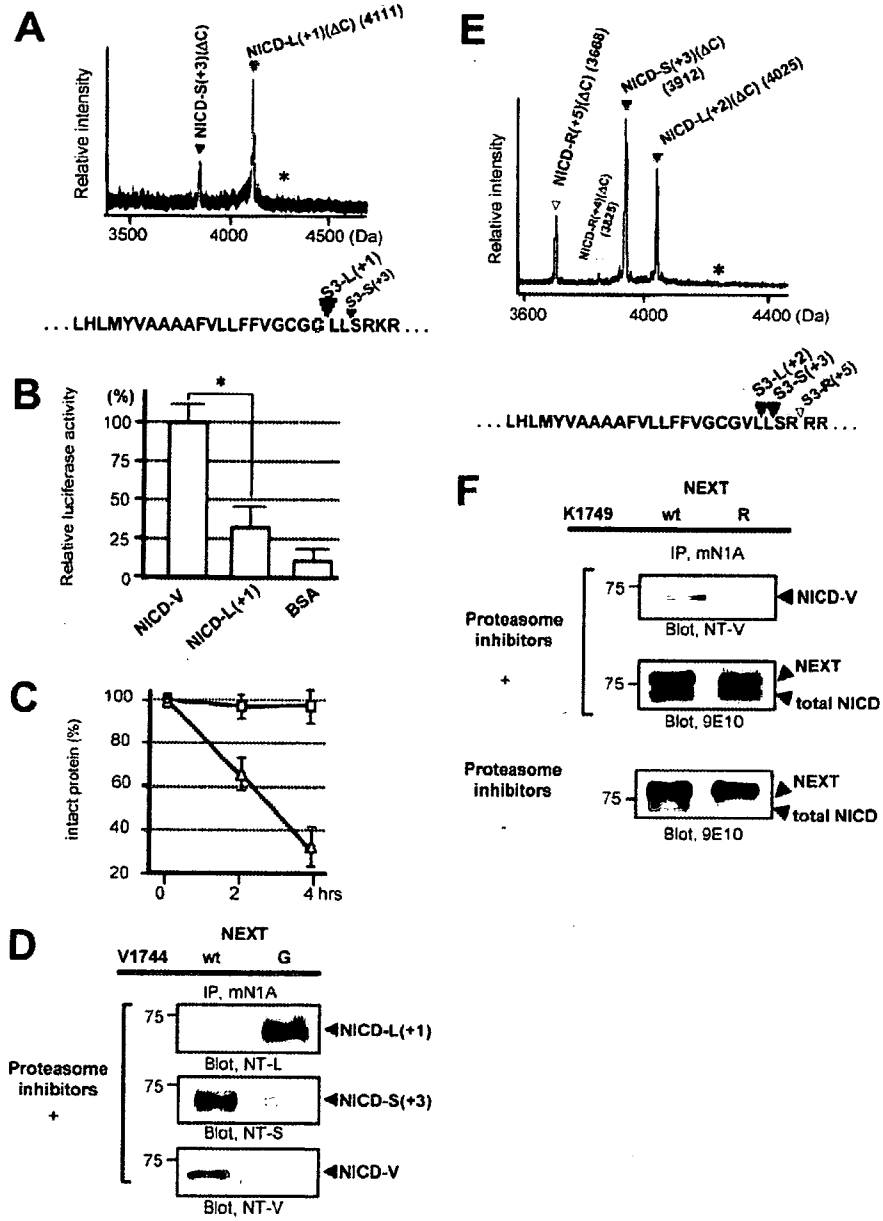

FIG. 8. Characteristics of the NICD species generated from the Val→Gly and the Lys→Arg mutants in cultured cells. (A) MS spectrum of de novo NICD(ΔC) generated from the Val→Gly mutant of NEXTΔC in K293 cells. The asterisk indicates the position of molecular mass corresponding to NICD-G(ΔC) species. Colored letters and inverted triangles show the mutation and proteolytic sites, respectively. (B) Assay of Notch downstream signaling induced by NICD-L(+1). Experiments were performed as described for Fig. 5B. The luciferase activity in the NICD-V-loaded cells was defined as 100%. Values represent means ± standard deviations. (n = 3). The asterisk indicates that the relative luciferase activity in NICD-V-loaded cells is statistically different than that in NICD-L(+1)-loaded cells ($P < 0.001$). (C) Degradation of NICD-L(+1) species in vitro. Experiments were performed as described for Fig. 5C but using NICD-L(+1) (triangles) and NICD-V (squares). Values represent means ± standard deviations (n = 3). (D) Generation of NICD-L(+1) and NICD-S(+3) in the Val→Gly mutant NEXT cells. K293 cells expressing either wt or the Val→Gly mutant NEXT were analyzed as described for Fig. 2D. (E) MS spectrum of de novo NICD(ΔC) generated from the Lys→Arg mutant of NEXTΔC in K293 cells. The asterisk indicates the position of molecular mass corresponding to NICD-V(ΔC) species. Colored letters and inverted triangles show the mutation and proteolytic sites, respectively. (F) Generation of unstable NICD species in the Lys→Arg mutant NEXT cells. K293 cells expressing either wt or the Lys→Arg mutant NEXT were analyzed as described for Fig. 2D (top and middle panels).

least partially responsible for the observed decrease in NICD level/Notch signaling in cultured cells.

Unlike several FAD-associated PS1 mutations, modifiers of PS/γ-secretase do not induce changes in the precision of S3 cleavage. Many FAD PS mutations affect the precision of not only γ but also ε cleavages of βAPP and, therefore, generally increase the relative AICDε48/AICDε49 ratio as well as the Aβ42/Aβ40 ratio (38, 42). In addition, compounds that modify the activity of PS/γ-secretase, including a subset of nonsteroidal anti-inflammatory drugs, cause reciprocal changes in rela-

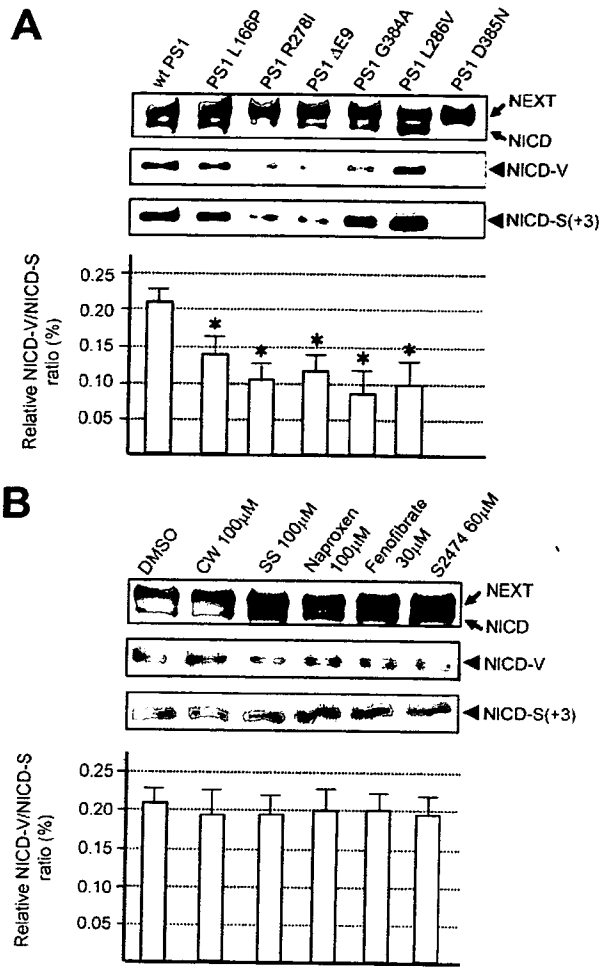

FIG. 9. Changes in the precision of S3 cleavage induced by FAD mutations in PS1. (A) Effect of several FAD PS1 mutations on the precision of S3 cleavage. K293 cells expressing the indicated PS mutant were transiently transfected with NEXT and analyzed as for Fig. 2D. The production of total NICD (first panel), NICD-V (second panel), and NICD-S(+3) (third panel) was assessed. Note that amount of total NICD was greatly reduced in PS1 R278I- and Δexon 9-expressing cells. The ratio of NICD-V to NICD-S(+3) in cells expressing wt PS1 or FAD mutants is shown in the bottom panel. Values represent means ± standard deviations (n = 3). The asterisk indicates that the ratio of NICD-V to NICD-S(+3) in cells expressing PS1 FAD mutants is significantly different from that in wt PS1-expressing cells ($P < 0.002$). (B) Effect of PS/γ-secretase modifiers on the precision of S3 cleavage. K293 cells stably expressing NEXT were treated with several PS/γ-secretase modifiers at the indicated concentration for 24 h and analyzed as described for the first three panels in panel A. DMSO, dimethyl sulfoxide; CW, compound W (31); SS, sulindac sulfide (49). The ratio of NICD-V to NICD-S(+3) in the control and treated cells is shown in the bottom panel. Values represent means ± standard deviations (n = 3).

tive production of Aβ42 and Aβ38 (19, 31, 49). Therefore, we investigated whether FAD PS mutations or PS/γ-secretase modifiers affect the precision of S3 cleavage. To evaluate the precision change, we used the relative NICD-V/NICD-S ratio, mimicking the relative Aβ42/Aβ40 ratio in the case of γ cleavage. Immunoblotting using anti-NT-V or anti-NT-S revealed that cells coexpressing PS1 mutants and NEXT produce both of the NICD species (Fig. 9A, top three panels). We found that the relative ratio of S3-V to S3-S(+3) cleavage was significantly reduced in some mutants (Fig. 9A, bottom panel). Subsequently, we examined the effects of PS/γ-secretase modifiers and naproxen (Fig. 9B). Because the effective doses of the compounds for γ and S3 cleavage may differ, we performed dose-response experiments to select the highest working concentrations (data not shown). After confirming that the level of Aβ42 in the medium was altered following a 24-h incubation with each compound (data not shown), we analyzed the cell lysates for the presence of NICD-V and NICD-S(+3) (Fig. 9B). In contrast to the case for the FAD mutants, the relative ratio of S3-V to S3-S(+3) cleavage was unchanged by the modifiers. These results suggest that γ-secretase modifiers do not affect the precision of intramembrane proteolysis by PS/γ-secretase.

DISCUSSION

The current studies suggest a novel mode by which the intensity of Notch signaling is regulated. We found that intracellular Notch signaling molecules (NICDs) in target cells can be divided into a stable one that transmits a substantial signal and unstable ones that transmit a much weaker signal, depending on the specific site of S3 cleavage. Therefore, Notch signaling intensity transmitted by conversion of extracellular signaling into intracellular signaling could depend on the characteristics of the target cell. For example, although S3 cleavage occurs, cells might not receive a substantial Notch signal when predominantly unstable NICDs are generated. On the basis of our results, we propose that the precision of S3 cleavage by PS/γ-secretase in the target cell is an important factor in determining the signaling intensity.

PS-dependent proteolysis on the TM of Notch-1 and βAPP consists of dual cleavage at the S4/S3 and γ/ε sites, respectively (14, 31, 33). The finding of diversity in the site of S3 cleavage means that cleavage at all four sites in the TM of Notch-1 and βAPP can vary. Thus, we suggest that the existence of variability in both the site and precision of cleavage may be a common feature of PS-dependent intramembrane proteolysis. Furthermore, we found that the precision of cleavage at S3 changes according to the subcellular location. On the PM, cleavage is more likely at S3-V, whereas on endosomes, cleavage is more likely at S3-S(+3), which is more C terminal. Interestingly, we have obtained very similar results regarding the cleavage of βAPP at the ε site (11). The precision of cleavage at the ε site changes depending on the subcellular location (11). The ε49 cleavage, which topologically corresponds to S3-V, occurs mainly on the PM, whereas the more C-terminal ε51 cleavage, which topologically corresponds to S3-S, occurs mainly on endosomes. Therefore, we have demonstrated that such subcellular location-dependent changes in the precision of the cleavage by PS/γ-secretase are common to the substrates. These findings suggest that such changes reflect a functional alteration of PS/γ-secretase in each subcellular location.

S2 cleavage upon ligand binding should occur on the PM of the target cells, but whether the subsequent S3 cleavage occurs on the PM or after endocytosis remains controversial (13, 17, 20, 46). The results of the current study suggest that (i) S3 cleavage occurs in both subcellular fractions in cell culture and

(ii) S3-V cleavage, which generates stable NICD-V, occurs predominantly on the PM, whereas S3-S(+3) cleavage, which generates unstable NICD-S(+3), occurs predominantly on endosomes. We also found that the intensity of Notch signaling changes along with the extent of endocytosis, perhaps due to a change in the precision of S3 cleavage. Therefore, our results suggest that NICD generation on the PM and endosomes increases and decreases the intensity of Notch signaling, respectively. Reports that Sanpodo positively regulates Notch signaling on the PM and that Numb, a negative regulator, promotes endocytosis of Notch receptors and/or Sanpodo are consistent with our findings (3, 28). A previous study showed that *Drosophila* with a mutation in *shibire*, which encodes a homolog of dynamin, has a phenotype indicating a loss of Notch function (43). Further study to solve the contradiction is necessary.

Elimination of either Notch or PS function causes a strong Notch loss-of-function phenotype in vivo (23, 41). Knock-in mice with the S3 (Val→Gly) mutant of Notch-1 display a hypomorphic Notch phenotype, possibly due to reduced Notch signaling caused by a decrease in the intracellular NICD level (6, 15, 39). This reduction in the level of NICD polypeptides could be due to decreased generation and/or increased degradation (4, 6). Previously, NICD was considered to be a single polypeptide mediating a single type of signaling, implying that the lower level of NICD is due to a decrease in its generation; however, we found that the N termini of NICDs may play critical roles in their stabilities and thus signaling intensities.

Among S3 mutants of Notch-1, the Lys→Arg mutant NEXT is neither monoubiquitinated at Arg1749 nor endocytosed (13). Concurrently, the NICD-V level in the cells expressing this mutant is low (13). In this paper, we demonstrated that the Lys→Arg mutation also causes a drastic change in the precision of the S3 cleavage, which results in a drastic decrease of NICD-V generation on the PM. This explanation, if valid, resolves the discrepancy between the two studies.

Both stabilizing (Val, Met, or Gly) and destabilizing amino acid residues seem to be conserved in Notch orthologs of various organisms (see Table S2 in the supplemental material). This suggests that both stable and unstable intracellular Notch signaling exists in many species. Previous studies have indicated that differences in the intensity, duration, and timing of Notch signaling in target cells affect cell fate decisions (7, 26). Furthermore, the signaling by a molecule is dependent on its lifetime in the cell, and the lifetime should be short enough for the target cell to be able to rapidly change the extent of signaling (22). Therefore, target cells in different contexts may convert extracellular signals to various relative amounts of short- and long-term Notch signals.

FAD PS mutations generally increase the generation of Aβ42 (42). This pathological gain of function of PS is due to a change in the precision of γ cleavage, resulting in an increase in cleavage at γ42 (42). PS/γ-secretase modifiers can up- or down-regulate the cleavage at γ42 (19, 31, 49). In both cases, the modifiers have reciprocal effects on the production of Aβ42 and Aβ38 (31, 49). In this study, we found that several FAD PS1 mutants change the precision of S3 cleavage but that the PS/γ-secretase modifiers do not. These findings are consistent with previous studies showing that the precision of ε cleavage in βAPP is altered by certain FAD PS mutations (38) and that Notch processing is unaffected by nonsteroidal anti-inflammatory drugs that can reduce Aβ42 generation (45, 49). PS/γ-secretase modifiers could thus affect the precision of the intramembrane proteolysis differently from PS FAD mutations.

Because up-regulation in Notch signaling is involved in a subset of malignancies (10, 37, 47, 50), γ-secretase inhibitors have been considered for the treatment of cancer; however, inhibitors would cause the accumulation of substrates (i.e., NEXT), inevitably producing a "rebound effect," where the concentration of NICD would increase. Therefore, compounds that alter the precision of S3 cleavage and specifically inhibit the generation of stable NICD-V may be more effective therapeutic agents.

ACKNOWLEDGMENTS

We thank J. Takeda, R. Kopan, M. Nishimura, H. Hasegawa, Y. Eguchi, Y. Tsujimoto, H. Steiner, and C. Haass for critically reading the manuscript and S. Shirahata, R. Kopan, J. S. Nye, A. Israel, S. L. Schmid, and G. W. Bornkamm for providing cDNAs, constructs, and cell lines.

M.O. conceived and designed the experiments. S.T. and others performed the experiments. M.O. wrote the paper.

We are grateful for funding from the Program for the Promotion of Fundamental Studies in Health Sciences of the National Institute of Biomedical Innovation (05-26) (to M.T., M.O., and S.T.), grants-in-aid for Scientific Research on Priority Areas-Advanced Brain Science Project (to M.O.) and KAKEN-HI from the Ministry of Education, Culture, Sports, Science, and Technology (to M.T., M.O., and S.T.), and grants-in-aid from the Japanese Ministry of Health, Labor and Welfare (to M.T. and M.O.).

We declare that no competing interests exist.

REFERENCES

1. **Artavanis-Tsakonas, S., M. D. Rand, and R. J. Lake.** 1999. Notch signaling: cell fate control and signal integration in development. Science **284**:770–776.
2. **Bachmair, A., D. Finley, and A. Varshavsky.** 1986. In vivo half-life of a protein is a function of its amino-terminal residue. Science **234**:179–186.
3. **Berdnik, D., T. Torok, M. Gonzalez-Gaitan, and J. A. Knoblich.** 2002. The endocytic protein alpha-adaptin is required for numb-mediated asymmetric cell division in Drosophila. Dev. Cell **3**:221–231.
4. **Blat, Y., J. E. Meredith, Q. Wang, J. D. Bradley, L. A. Thompson, R. E. Olson, A. M. Stern, and D. Seiffert.** 2002. Mutations at the P1′ position of Notch1 decrease intracellular domain stability rather than cleavage by gamma-secretase. Biochem. Biophys. Res. Commun. **299**:569–573.
5. **Cao, X., and T. C. Sudhof.** 2001. A transcriptionally active complex of APP with Fe65 and histone acetyltransferase Tip60. Science **293**:115–120.
6. **Chandu, D., S. S. Huppert, and R. Kopan.** 2006. Analysis of transmembrane domain mutants is consistent with sequential cleavage of Notch by gamma-secretase. J. Neurochem. **96**:228–235.
7. Reference deleted.
8. **De Strooper, B., W. Annaert, P. Cupers, P. Saftig, K. Craessaerts, J. S. Mumm, E. H. Schroeter, V. Schrijvers, M. S. Wolfe, W. J. Ray, A. Goate, and R. Kopan.** 1999. A presenilin-1-dependent gamma-secretase-like protease mediates release of Notch intracellular domain. Nature **398**:518–522.
9. **Fehon, R. G., K. Johansen, I. Rebay, and S. Artavanis-Tsakonas.** 1991. Complex cellular and subcellular regulation of notch expression during embryonic and imaginal development of Drosophila: implications for notch function. J. Cell Biol. **113**:657–669.
10. **Fre, S., M. Huyghe, P. Mourikis, S. Robine, D. Louvard, and S. Artavanis-Tsakonas.** 2005. Notch signals control the fate of immature progenitor cells in the intestine. Nature **435**:964–968.
11. **Fukumori, A., M. Okochi, S. Tagami, J. Jiang, N. Itoh, T. Nakayama, K. Yanagida, Y. Ishizuka-Katsura, T. Morihara, K. Kamino, T. Tanaka, T. Kudo, H. Tanii, A. Ikuta, C. Haass, and M. Takeda.** 2006. Presenilin-dependent gamma-secretase on plasma membrane and endosomes is functionally distinct. Biochemistry **45**:4907–4914.
12. **Gonda, D. K., A. Bachmair, I. Wunning, J. W. Tobias, W. S. Lane, and A. Varshavsky.** 1989. Universality and structure of the N-end rule. J. Biol. Chem. **264**:16700–16712.
13. **Gupta-Rossi, N., E. Six, O. LeBail, F. Logeat, P. Chastagner, A. Olry, A. Israel, and C. Brou.** 2004. Monoubiquitination and endocytosis direct gamma-secretase cleavage of activated Notch receptor. J. Cell Biol. **166**:73–83.

14. **Haass, C., and H. Steiner.** 2002. Alzheimer disease gamma-secretase: a complex story of GxGD-type presenilin proteases. Trends Cell Biol. **12**:556–562.
15. **Huppert, S. S., A. Le, E. H. Schroeter, J. S. Mumm, M. T. Saxena, L. A. Milner, and R. Kopan.** 2000. Embryonic lethality in mice homozygous for a processing-deficient allele of Notch1. Nature **405**:966–970.
16. **Jarriault, S., C. Brou, F. Logeat, E. H. Schroeter, R. Kopan, and A. Israel.** 1995. Signalling downstream of activated mammalian Notch. Nature **377**: 355–358.
17. **Kaether, C., S. Schmitt, M. Willem, and C. Haass.** 2006. Amyloid precursor protein and Notch intracellular domains are generated after transport of their precursors to the cell surface. Traffic **7**:408–415.
18. **Koo, E. H., and R. Kopan.** 2004. Potential role of presenilin-regulated signaling pathways in sporadic neurodegeneration. Nat. Med. **10**(Suppl.):S26–S33.
19. **Kukar, T., M. P. Murphy, J. L. Eriksen, S. A. Sagi, S. Weggen, T. E. Smith, T. Ladd, M. A. Khan, R. Kache, J. Beard, M. Dodson, S. Merit, V. V. Ozols, P. Z. Anastasiadis, P. Das, A. Fauq, E. H. Koo, and T. E. Golde.** 2005. Diverse compounds mimic Alzheimer disease-causing mutations by augmenting Abeta42 production. Nat. Med. **11**:545–550.
20. **Lopez-Schier, H., and D. St. Johnston.** 2002. Drosophila nicastrin is essential for the intramembranous cleavage of notch. Dev. Cell **2**:79–89.
21. **Minoguchi, S., Y. Taniguchi, H. Kato, T. Okazaki, L. J. Strobl, U. Zimber-Strobl, G. W. Bornkamm, and T. Honjo.** 1997. RBP-L, a transcription factor related to RBP-Jκ. Mol. Cell. Biol. **17**:2679–2687.
22. **Morimoto, M., Y. Takahashi, M. Endo, and Y. Saga.** 2005. The Mesp2 transcription factor establishes segmental borders by suppressing Notch activity. Nature **435**:354–359.
23. **Mumm, J. S., and R. Kopan.** 2000. Notch signaling: from the outside in. Dev. Biol. **228**:151–165.
24. **Mumm, J. S., E. H. Schroeter, M. T. Saxena, A. Griesemer, X. Tian, D. J. Pan, W. J. Ray, and R. Kopan.** 2000. A ligand-induced extracellular cleavage regulates gamma-secretase-like proteolytic activation of Notch1. Mol. Cell **5**:197–206.
25. **Munter, L. M., P. Voigt, A. Harmeier, D. Kaden, K. E. Gottschalk, C. Weise, R. Pipkorn, M. Schaefer, D. Langosch, and G. Multhaup.** 2007. GxxxG motifs within the amyloid precursor protein transmembrane sequence are critical for the etiology of Abeta42. EMBO J. **26**:1702–1712.
26. **Nakagawa, M., M. Ichikawa, K. Kumano, S. Goyama, M. Kawazu, T. Asai, S. Ogawa, M. Kurokawa, and S. Chiba.** 2006. AML1/Runx1 rescues Notch1-Null mutation-induced deficiency of para-aortic splanchnopleural hematopoiesis. Blood **108**:3329–3334.
27. **Nakaya, Y., T. Yamane, H. Shiraishi, H. Q. Wang, E. Matsubara, T. Sato, G. Dolios, R. Wang, B. De Strooper, M. Shoji, H. Komano, K. Yanagisawa, Y. Ihara, P. Fraser, P. St George-Hyslop, and M. Nishimura.** 2005. Random mutagenesis of presenilin-1 identifies novel mutants exclusively generating long amyloid beta-peptides. J. Biol. Chem. **280**:19070–19077.
28. **O'Connor-Giles, K. M., and J. B. Skeath.** 2003. Numb inhibits membrane localization of Sanpodo, a four-pass transmembrane protein, to promote asymmetric divisions in Drosophila. Dev. Cell **5**:231–243.
29. **Ohashi, H., and T. Sudo.** 1994. Efficient expression of a transfected foreign gene by Cos1 cells in serum-free medium. Biosci. Biotechnol. Biochem. **58**:758–759.
30. **Okochi, M., S. Eimer, A. Bottcher, R. Baumeister, H. Romig, J. Walter, A. Capell, H. Steiner, and C. Haass.** 2000. A loss of function mutant of the presenilin homologue SEL-12 undergoes aberrant endoproteolysis in Caenorhabditis elegans and increases abeta 42 generation in human cells. J. Biol. Chem. **275**:40925–40932.
31. **Okochi, M., A. Fukumori, J. Jiang, N. Itoh, R. Kimura, H. Steiner, C. Haass, S. Tagami, and M. Takeda.** 2006. Secretion of the Notch-1 Abeta-like peptide during Notch signaling. J. Biol. Chem. **281**:7890–7898.
32. **Okochi, M., K. Ishii, M. Usami, N. Sahara, F. Kametani, K. Tanaka, P. E. Fraser, M. Ikeda, A. M. Saunders, L. Hendriks, S. I. Shoji, L. E. Nee, J. J. Martin, C. Van Broeckhoven, P. H. St George-Hyslop, A. D. Roses, and H. Mori.** 1997. Proteolytic processing of presenilin-1 (PS-1) is not associated with Alzheimer's disease with or without PS-1 mutations. FEBS Lett. **418**: 162–166.
33. **Okochi, M., H. Steiner, A. Fukumori, H. Tanii, T. Tomita, T. Tanaka, T. Iwatsubo, T. Kudo, M. Takeda, and C. Haass.** 2002. Presenilins mediate a dual intramembranous gamma-secretase cleavage of Notch-1. EMBO J. **21**: 5408–5416.
34. **Okochi, M., J. Walter, A. Koyama, S. Nakajo, M. Baba, T. Iwatsubo, L. Meijer, P. J. Kahle, and C. Haass.** 2000. Constitutive phosphorylation of the Parkinson's disease associated alpha-synuclein. J. Biol. Chem. **275**:390–397.
35. **Parks, A. L., K. M. Klueg, J. R. Stout, and M. A. Muskavitch.** 2000. Ligand endocytosis drives receptor dissociation and activation in the Notch pathway. Development **127**:1373–1385.
36. **Qi-Takahara, Y., M. Morishima-Kawashima, Y. Tanimura, G. Dolios, N. Hirotani, Y. Horikoshi, F. Kametani, M. Maeda, T. C. Saido, R. Wang, and Y. Ihara.** 2005. Longer forms of amyloid beta protein: implications for the mechanism of intramembrane cleavage by gamma-secretase. J. Neurosci. **25**:436–445.
37. **Radtke, F., and K. Raj.** 2003. The role of Notch in tumorigenesis: oncogene or tumour suppressor? Nat. Rev. Cancer **3**:756–767.
38. **Sato, T., N. Dohmae, Y. Qi, N. Kakuda, H. Misonou, R. Mitsumori, H. Maruyama, E. H. Koo, C. Haass, K. Takio, M. Morishima-Kawashima, S. Ishiura, and Y. Ihara.** 2003. Potential link between amyloid beta-protein 42 and C-terminal fragment gamma 49–99 of beta-amyloid precursor protein. J. Biol. Chem. **278**:24294–24301.
39. **Schroeter, E. H., J. A. Kisslinger, and R. Kopan.** 1998. Notch-1 signalling requires ligand-induced proteolytic release of intracellular domain. Nature **393**:382–386.
40. **Schweisguth, F.** 2004. Notch signaling activity. Curr. Biol. **14**:R129–R138.
41. **Selkoe, D., and R. Kopan.** 2003. Notch and Presenilin: regulated intramembrane proteolysis links development and degeneration. Annu. Rev. Neurosci. **26**:565–597.
42. **Selkoe, D. J.** 2001. Alzheimer's disease: genes, proteins, and therapy. Physiol. Rev. **81**:741–766.
43. **Seugnet, L., P. Simpson, and M. Haenlin.** 1997. Requirement for dynamin during Notch signaling in Drosophila neurogenesis. Dev. Biol. **192**:585–598.
44. **Steiner, H., M. Kostka, H. Romig, G. Basset, B. Pesold, J. Hardy, A. Capell, L. Meyn, M. L. Grim, R. Baumeister, K. Fechteler, and C. Haass.** 2000. Glycine 384 is required for presenilin-1 function and is conserved in bacterial polytopic aspartyl proteases. Nat. Cell Biol. **2**:848–851.
45. **Takahashi, Y., I. Hayashi, Y. Tominari, K. Rikimaru, Y. Morohashi, T. Kan, H. Natsugari, T. Fukuyama, T. Tomita, and T. Iwatsubo.** 2003. Sulindac sulfide is a noncompetitive gamma-secretase inhibitor that preferentially reduces Abeta 42 generation. J. Biol. Chem. **278**:18664–18670.
46. **Tarassishin, L., Y. I. Yin, B. Bassit, and Y. M. Li.** 2004. Processing of Notch and amyloid precursor protein by gamma-secretase is spatially distinct. Proc. Natl. Acad. Sci. USA **101**:17050–17055.
47. **van Es, J. H., M. E. van Gijn, O. Riccio, M. van den Born, M. Vooijs, H. Begthel, M. Cozijnsen, S. Robine, D. J. Winton, F. Radtke, and H. Clevers.** 2005. Notch/gamma-secretase inhibition turns proliferative cells in intestinal crypts and adenomas into goblet cells. Nature **435**:959–963.
48. **Washburn, T., E. Schweighoffer, T. Gridley, D. Chang, B. J. Fowlkes, D. Cado, and E. Robey.** 1997. Notch activity influences the alphabeta versus gammadelta T cell lineage decision. Cell **88**:833–843.
49. **Weggen, S., J. L. Eriksen, P. Das, S. A. Sagi, R. Wang, C. U. Pietrzik, K. A. Findlay, T. E. Smith, M. P. Murphy, T. Bulter, D. E. Kang, N. Marquez-Sterling, T. E. Golde, and E. H. Koo.** 2001. A subset of NSAIDs lower amyloidogenic Abeta42 independently of cyclooxygenase activity. Nature **414**:212–216.
50. **Weng, A. P., A. A. Ferrando, W. Lee, J. P. t. Morris, L. B. Silverman, C. Sanchez-Irizarry, S. C. Blacklow, A. T. Look, and J. C. Aster.** 2004. Activating mutations of NOTCH1 in human T cell acute lymphoblastic leukemia. Science **306**:269–271.
51. **Wolfe, M. S., W. Xia, B. L. Ostaszewski, T. S. Diehl, W. T. Kimberly, and D. J. Selkoe.** 1999. Two transmembrane aspartates in presenilin-1 required for presenilin endoproteolysis and gamma-secretase activity. Nature **398**: 513–517.
52. **Xia, W., and M. S. Wolfe.** 2003. Intramembrane proteolysis by presenilin and presenilin-like proteases. J. Cell Sci. **116**:2839–2844.
53. **Zhao, G., M. Z. Cui, G. Mao, Y. Dong, J. Tan, L. Sun, and X. Xu.** 2005. Gamma-cleavage is dependent on zeta-cleavage during the proteolytic processing of amyloid precursor protein within its transmembrane domain. J. Biol. Chem. **280**:37689–37697.

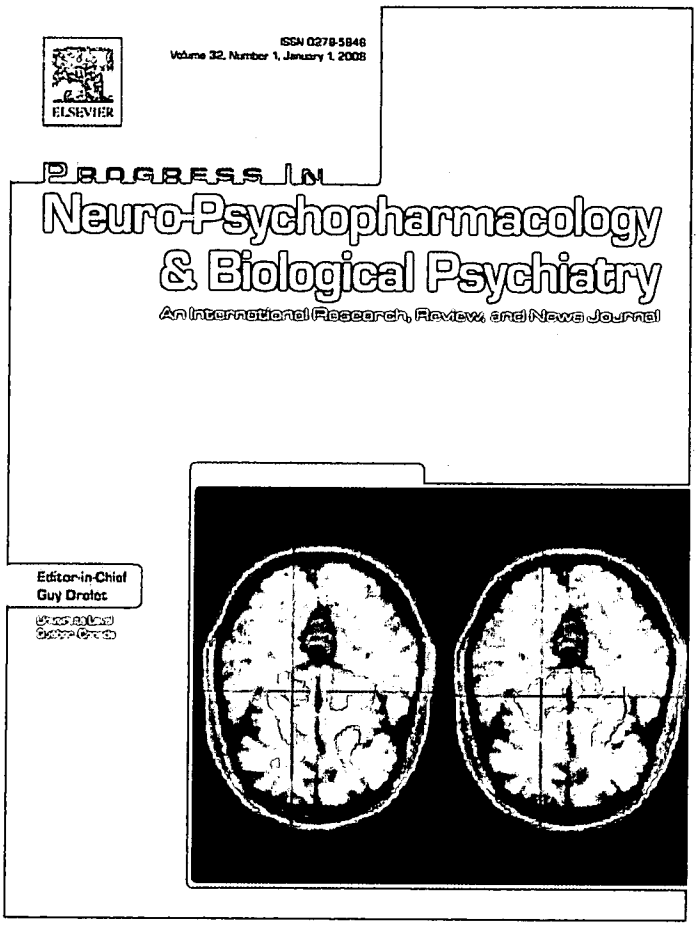

Available online at www.sciencedirect.com
ScienceDirect
Progress in Neuro-Psychopharmacology & Biological Psychiatry 32 (2008) 204–208
Progress in Neuro-Psychopharmacology & Biological Psychiatry
www.elsevier.com/locate/pnpbp

A possible association between missense polymorphism of the breakpoint cluster region gene and lithium prophylaxis in bipolar disorder

Takuya Masui [a], Ryota Hashimoto [b,c,d,*], Ichiro Kusumi [a], Katsuji Suzuki [a], Teruaki Tanaka [a], Shin Nakagawa [a], Tatsuyo Suzuki [e], Nakao Iwata [e], Norio Ozaki [f], Tadafumi Kato [g], Masatoshi Takeda [b,c], Hiroshi Kunugi [d], Tsukasa Koyama [a]

[a] *Department of Psychiatry, Hokkaido University Graduate School of Medicine, Kita 15 Nishi 7, Kita-ku, Sapporo, 060-8638, Hokkaido, Japan*
[b] *The Osaka-Hamamatsu Joint Research Center For Child Mental Development, Osaka University Graduate school of Medicine, D3, 2-2, Yamadaoka, Suita, Osaka, 565-0871, Japan*
[c] *Department of Psychiatry, Osaka University Graduate school of Medicine, Japan*
[d] *Department of Mental Disorder Research, National Institute of Neuroscience, National Center of Neurology and Psychiatry, 4-1-1, Ogawahigashicho, Kodaira, Tokyo, 187-8502, Japan*
[e] *Department of Psychiatry, Fujita Health University School of Medicine, 1-98 Dengakugakubo, Kutsukake-cho, Toyoake, Aichi, 470-1192, Japan*
[f] *Department of Psychiatry, Nagoya University Graduate School of Medicine, 65 Tsuruma-cho, Showa-ku, Nagoya, 466-8550, Japan*
[g] *Laboratory for Molecular Dynamics of Mental Disorders Brain Science Institute, RIKEN, 2-1 Hirosawa, Wako, Saitama, 351-0198, Japan*

Received 4 February 2007; received in revised form 13 August 2007; accepted 13 August 2007
Available online 19 August 2007

Abstract

Lithium is one of the most commonly used drugs for the treatment of bipolar disorder. To prescribe lithium appropriately to patients, predictors of response to this drug were explored, and several genetic markers are considered to be good candidates. We previously reported a significant association between genetic variations in the breakpoint cluster region (BCR) gene and bipolar disorder. In this study, we examined a possible relationship between response to maintenance treatment of lithium and Asn796Ser single-nucleotide polymorphism in the BCR gene. Genotyping was performed in 161 bipolar patients who had been taking lithium for at least 1 year, and they were classified into responders for lithium monotherapy and non-responders. We found that the allele frequency of Ser796 was significantly higher in non-responders than in responders. Further investigation is warranted to confirm our findings.

Keywords: BCR (breakpoint cluster region); Bipolar disorder; Lithium; SNP (single-nucleotide polymorphism)

1. Introduction

Bipolar disorder (BPD) is one of the most distinct syndromes in psychiatry, which is characterized by recurrent episodes of mania and depression. Three representative mood stabilizers, lithium, valproate and carbamazepine, are used worldwide for its treatment, and American Psychiatric Association guideline listed lithium as a first line agent (American Psychiatric Association, 2002). However, these treatments are associated with variable rates of efficacy and often with intolerable side effects. Therefore, many researchers explored psychopathological and biological markers for good response to lithium treatment (Gelenberg and Pies, 2003; Ikeda and Kato, 2003). To date, several studies investigated possible molecular predictors of lithium efficacy. The functional polymorphism in the upstream regulatory region of the serotonin transporter gene (5-HTTLPR) has been associated with lithium efficacy in two independent studies (Serretti et al., 2001;

Abbreviations: ANOVA, analysis of variance; BCR, breakpoint cluster region; BDNF, brain-derived neurotrophic factor; BPD, bipolar disorder; BP I, bipolar I disorder; BP II, bipolar II disorder; PH domain, pleckstrin homology domain; SNP, single-nucleotide polymorphism.

* Corresponding author. The Osaka-Hamamatsu Joint Research Center For Child Mental Development, Osaka University Graduate school of Medicine, D3, 2-2, Yamadaoka, Suita, Osaka, 565-0871, Japan. Tel.: +81 6 6879 3074; fax: +81 6 6879 3059.
E-mail address: hashimor@psy.med.osaka-u.ac.jp (R. Hashimoto).

0278-5846/$ - see front matter © 2007 Elsevier Inc. All rights reserved.
doi:10.1016/j.pnpbp.2007.08.010

Del Zompo et al., 1999), although the polymorphism associated with better lithium response was opposite. Other numerous genetic variants including catechol-*O*-methyltransferase were not associated with lithium response (Serretti et al., 2002). The association between prophylactic lithium response and the polymorphism of the brain-derived neurotrophic factor (BDNF) gene was reported (Rybakowski et al., 2005); however, this association was not replicated in subsequent studies (Masui et al., 2006; Michelon et al., 2006).

We previously reported a significant association between genetic variants in the breakpoint cluster region gene (*BCR*), which is located on chromosome 22q11, and BPD (Hashimoto et al., 2005). The *BCR* is highly expressed in hippocampal pyramidal cell layer and dentate gyrus (Fioretos et al., 1995), and encodes a Rho GTPase-activating protein (GAP), which inactivate the Rho GTPase playing an important role in neuronal development (Diekmann et al., 1991; Negishi and Katoh, 2002). The A2387G single-nucleotide polymorphism (SNP) in the *BCR* gene [National Center for Biotechnology Information (NCBI) SNP ID: rs140504] is the non-conservative SNP giving rise to an amino acid change of asparagine to serine at codon 796 (Asn796Ser; NCBI Protein ID: NP_004318). Ser796 allele showed a significant association with BPD and stronger evidence for an association with bipolar II disorder (BPII) than bipolar I disorder (BPI) (Hashimoto et al., 2005). It has been reported that patients with BPII have greater number of abnormal mood episodes and comorbidity of other psychiatric illnesses than patients with BPI (Ayuso-Gutierrez and Ramos-Brieva, 1982; Berk and Dodd, 2005). These clinical features of BPII have been also considered as markers for poor response to lithium treatment (Ikeda and Kato, 2003). Therefore, Ser796 allele of the *BCR* gene may contribute to poorer response to lithium therapy in BPD.

In this study, we examined the possible association between prophylactic effect of lithium and Asn796Ser SNP of the *BCR* gene in Japanese patients with BPD.

2. Methods

2.1. Subjects

Subjects were 161 patients with BPD (83 patients were BPI, and 78 patients were BPII). Consensus diagnosis was made for each patient by at least two psychiatrists according to the Diagnostic and Statistical Manual of Mental Disorders 4th edition (DSM-IV) criteria. The presence of concomitant diagnoses of mental retardation, drug dependence, or other Axis I disorder, together with somatic or neurological illnesses that impaired psychiatric evaluation, represented exclusion criteria. They were composed of 76 males and 85 females with mean age of 48.2± 12.8 years (mean±S.D.). All the subjects were biologically unrelated Japanese. Patients had been treated with lithium carbonate and its serum concentration was maintained between 0.4 and 1.2 mEq/L at least for one year, in a completely naturalistic setting.

Response to lithium treatment was retrospectively determined for each patient from all available information including clinical interview and medical records, by at least two psychiatrists, and the patients were classified into lithium responders and non-responders. The phenotype definition of lithium prophylaxis is a very difficult issue. Lithium responders were defined as those patients without any affective episodes during the maintenance period of lithium mono-therapy. During the maintenance period, the addition of antidepressants, antipsychotics, or anticonvulsants was regarded as a relapse, and excluded from the responder group. However, coadministration of hypnotics for sleep disturbance was allowed, and was not regarded as a relapse when subsequent affective episode did not appear.

Our definition of response to lithium treatment is full response without any affective episode during lithium treatment. This definition is similar to "excellent lithium responders" used as clinical endophenotypic marker of BPD in some molecular-genetic research (Rybakowski et al., 2005; Mamdani et al., 2007). On the other hand, recurrence index [number of episodes/duration of illness (years)] before and during lithium treatment is a better method to measure the response to lithium including partial response (Gasperini et al., 1993; Serretti et al., 2002). However, more clinical information is necessary to calculate the recurrence index. We investigated the association between the change of recurrence index and clinical variables in parts of total subjects (24 patients) whose recurrence pattern were clearly established during more than 1 year [mean 5.8±5.0 (range 1.3–21.0) years] before lithium treatment. They were composed of 9 BPI and 15 BPII patients, whose age of onset was 35.4± 9.5 years old, duration from onset of illness to lithium treatment was 9.5±7.0 (range 1.3–22.0) years, number of episodes which could be clearly identified before lithium treatment was 16.3± 30.3 (range 3.0–150.0), duration of lithium treatment was 6.0± 4.3 (range 1.0–14.3) years, number of episodes during lithium treatment was 6.8±6.0 (range 0.0–26.0) and recurrence index before and during lithium were 2.7±2.8 (range 0.6–14.2) and 1.8±1.5 (range 0.0–5.3), respectively.

After complete description of the study, written informed consent was obtained from every subject. The study protocol was approved by institutional ethics committees.

Table 1
Clinical characteristics of subjects, sorted by response to lithium treatment

	Response to lithium treatment		
	Responders (N=43)	Non-responders (N=118)	
Subtype			χ^2test
BPI	29 (34.9%)	54 (65.1%)	$p<0.05$
BPII	14 (18.0%)	64 (82.0%)	
Gender			
Male	25 (32.9%)	51 (67.1%)	NS
Female	18 (21.2%)	67 (78.8%)	
			t-test
Age at last observation	54.4±11.8	46.1±12.4	$p<0.01$
Age of onset	41.5±13.6	32.9±10.7	$p<0.01$
Duration of illness	12.9±9.0	13.2±9.9	NS

Continuous values were represented as the mean±SD.
BPI=bipolar I disorder, BPII=bipolar II disorder,
NS=not significant.

Table 2
Allele frequencies and genotype of the Asn796Ser polymorphism of the BCR gene and response to lithium treatment

Response to lithium treatment	Allele frequency		χ^2test	Genotype		χ^2test
	Asn	Ser	p value (OR)	Asn/Asn Asn/Ser	Ser/Ser	p value
Responders (n=43)	49 (57.0%)	37 (43.0%)		35 (81.4%)	8 (18.6%)	
Non-responders (n=118)	101 (42.8%)	135 (57.2%)		77 (65.3%)	41 (34.7%)	
			0.024 (1.77)			0.049
Total patients (n=161)	150 (46.6%)	172 (53.4%)		112 (69.6%)	49 (30.4%)	

OR: Odds ratio.

2.2. Genotyping

Venous blood was drawn from the subjects and genomic DNA was extracted from whole blood according to the standard procedures. The genotype of the Asn796Ser SNP (rs140504) of the *BCR* gene was determined by TaqMan 5′-exonuclease allelic discrimination assay, described previously (Hashimoto et al., 2005). Briefly, probes and primers for detection of the polymorphism were: forward primer 5′-AGCTGGACGCTTTGAAGATCA-3′, reverse primer 5′-TGGTGTGCACCTTCTCTCTCT-3′, probe 1 5′-VIC-CCAGATCAAGAATGACAT-MGB-3′, and probe 2 5′-FAM-CCAGATCAAGAGTGACAT-MGB-3′. PCR cycling conditions were: at 95 °C for 10 min, 50 cycles of 92 °C for 15 s and 60 °C for 1 min.

2.3. Statistical analysis

Difference in clinical characteristics between responders and non-responders to lithium treatment was analyzed using the χ^2 tests for categorical variables and t tests for continuous variables. The presence of Hardy–Weinberg equilibrium was examined by using the χ^2 test for goodness of fit. Subsequently, multiple logistic regression analysis was performed to correct background difference between responders and non-responders for lithium treatment. Possible predictors (genotype of the *BCR* gene, subtype of bipolar disorder, age of onset, age at last observation, and gender) were included in the original model. Backward stepwise regression was performed, and p-value greater than 0.10 was used for variable removal. Pearson coefficient of correlation test was used for comparison between recurrence index and clinical variables. The effect of the Asn796Ser SNP on recurrence index was assessed by analysis of variance (ANOVA). All p-values reported are two-tailed. Statistical significance was defined at $p<0.05$.

3. Results

Among 161 patients with BPD, 43 patients were determined as responders and 118 patients as non-responders for the maintenance treatment of lithium. The clinical characteristics sorted by response to lithium treatment and genotype distribution were presented in Table 1. There were significant differences between responders and non-responders in subtype of bipolar disorder (BPI and BPII), age at last observation, and age of onset.

The genotype distributions for the total patients, responders, and non-responders were in Hardy–Weinberg equilibrium (total patients: $\chi^2=0.94$, $df=1$, $p=0.33$; responders: $\chi^2<0.001$, $df=1$, $p=0.98$; non-responders: $\chi^2=0.81$, $df=1$, $p=0.37$). Allele frequencies and genotype distributions of the Asn769Ser polymorphism of the *BCR* gene among responders and non-responders for lithium treatment are presented in Table 2. The Ser796 allele was in excess in the non-responders rather than responders ($\chi^2=5.09$, $df=1$, $p=0.024$; OR 1.77, 95% CI 1.08–2.92). Then, we examined patients homozygous for the Ser796 allele and the Asn796 allele carriers, separately. Patients homozygous for the Ser796 allele were significantly more common in the non-responders than the Asn796 carriers ($\chi^2=3.88$, $df=1$, $p=0.049$; OR 2.33, 95% CI 0.99–5.49). After backward stepwise regression, the final logistic regression model included subtype of bipolar ($p<0.01$), age of onset ($p<0.01$), and genotype which is separated to the Asn796 carrier and homozygous for the Ser796 ($P=0.04$).

We next investigated the association between lithium response using recurrence index and clinical variables in 24 subjects with BPD. The change of recurrence index before to during lithium treatment was not associated with subtype (t=0.79, $df=22$, $p=0.44$), age of onset (correlation coefficient=−0.29, $p=0.17$), duration from onset of illness to lithium treatment (correlation coefficient=0.12, $p=0.57$), duration during treatment (correlation coefficient=0.11, $p=0.60$), or the Asn796Ser SNP ($df=2$, $F=0.03$, $p=0.97$).

We also examined the association between age of onset and recurrence index before lithium treatment, which reflects severity of illness. There was a negative trend between age of onset and recurrence index (correlation coefficient=−0.37, $p=0.074$). Although difference among genotype of Asn796Ser SNP was not statistically significant, the number of Ser796 allele was associated with higher recurrence index before lithium treatment (Asn/Asn=1.63±1.19, Asn/Ser=2.89±0.84, and Ser/Ser=3.23±1.19. $df=2$, $F=0.53$, $p=0.60$). Therefore, the Ser796 allele might also be associated with both early onset and severity of illness, which could result in poorer lithium response.

4. Discussion

We investigated a possible association between the *BCR* gene and the prophylactic effect of lithium treatment in patients with BPD for the first time. As expected, our results suggested that lithium treatment might be less effective in patients homozygous for the Ser796 allele of the *BCR* gene than in patients with the Asn796 allele. In addition, allele frequencies of the Ser796 associated with poorer lithium response were 43.0%

in responders and 57.2% in non-responders. As allele frequency of the Ser796 in healthy subjects in our previous study was 48.1% (Hashimoto et al., 2005), allele frequency of the Ser796 of responders is similar to the general population.

Comparing clinical characteristics of responders and non-responders, there were more BPII patients in non-responder group. Clinical characteristics predicting poorer response to lithium therapy and that of BPII seem to overlap each other, but better lithium response in BPI is not universally accepted. We excluded any Axis I comorbidity in this study. This would leave in more typical bipolar II patients who would be more likely to respond to lithium, however, other clinical factors such as Axis II comorbidity might influence our results. The presence of positive family history of lithium responsive BPD has been reported as indicative of favorable response (Grof et al., 2002). However, it was not assumed that our sample size was enough to investigate this issue because only 8.7% of BPD had positive family history of the same disease in 1st degree relatives (Smoller and Finn, 2003). Therefore, information about family history of lithium response was not collected in this study.

Age at onset was also different between responders and non-responders, and early age of onset was associated with poorer response to lithium treatment in our subjects. This observation is consistent with recent meta-analysis (Kleindienst et al., 2005). As the objective of this study is to examine the association between response to lithium treatment and a SNP in the *BCR* gene, the differences in demographic parameters of responders and non-responders might not be preferable. Therefore, we conducted a multiple logistic regression analysis, and homozygous for the Ser796 allele of the *BCR* gene was still significantly associated with poorer response to lithium treatment.

The evaluation of lithium prophylaxis is considerably difficult because of complex clinical course of BPD, and each researcher has used different methodologies. Although our finding was based on the simple definition, in which lithium responders didn't have any affective recurrences during lithium, one of the limitation of this study is lack of detailed clinical information, e.g. duration from onset of illness to lithium treatment and number of episodes which could be clearly identified before lithium treatment in total subjects. To evaluate lithium efficacy including partial response, calculating recurrence index before and during lithium treatment is used in several researches. This would be a correct measure of lithium prophylaxis, but evaluating mood recurrence accurately before the first contact to mental professionals is difficult. We tried to evaluate lithium response with recurrence index; however, we could examine it in only 24 subjects out of 161 subjects due to the difficulty of collecting this clinical information. We did not found any association between the recurrence index and clinical variables and the SNP in the *BCR* gene, except for the trend between the recurrence index and age of onset. As these results were from subgroup analysis with smaller number, further investigation is needed in a larger sample size.

In this study, the same variant associated with the illness was also associated with poorer outcome. This situation is similar to that of the Val allele of the *BDNF* Val66Met polymorphism (Rybakowski et al., 2005), and it is possible that the *BCR* Ser796 and the *BDNF* Val66 alleles are associated with severer illness presentation. The trend between the recurrence index and age of onset in our subgroup analysis might imply this possibility. In case of the *BDNF* Val66Met SNP, the functional differences arisen from each allele were reported (Eagan et al., 2003). While biological functional of the *BCR* Asn796Ser SNP is still unknown, this SNP may produce functional difference in the brain, like the *BDNF* Val66Met SNP. To speculate this issue, it is noteworthy that this SNP is in the pleckstrin homology (PH) domain of the *BCR*. As PH domain is known for its ability to bind phosphatidylinositol and this binding regulates the activity of PH domain containing protein (Lemmon et al., 2002), signal transduction from inositol cycle to the *BCR* products might be affected by this SNP. As the *BCR* is RhoGAP, this change may influence on the activity of its downstream target, RhoGTPase, which activates many kind of effectors associated with constructing neuronal network, and subsequently influence on neuronal development. Additionally, as inositol cycle is considered as one of therapeutic targets of lithium (Harwood, 2005), this SNP could alter the clinical efficacy of lithium. To understand the mechanism of our findings, it is worth investigating whether the Asn796Ser SNP alters the binding ability of PH domain to inositol.

5. Conclusion

This is the first report demonstrating that long-term lithium treatment may be less effective in BPD patients homozygous for Ser796 allele of the *BCR* gene than in patients with the Asn796 allele. The limitations of this study are retrospective design without placebo control group, small sample size, and lack of clinical information such as presence of rapid cycling and/or psychotic symptoms, and detailed lithium levels. Further investigations are needed to confirm our findings.

Acknowledgements

The authors thank Ms. Tomoko Shizuno and Keiko Okada for their technical assistance. This work was supported in part by Grants-in-Aid from the Japanese Ministry of Health, Labor and Welfare, the Japanese Ministry of Education, Culture, Sports, Science and Technology, CREST (Core research for Evolutional Science and Technology) of JST (Japan Science and Technology Agency), Research on Health Sciences focusing on Drug Innovation of The Japan Health Sciences Foundation, and Japan Foundation for Neuroscience and Mental Health.

Duality of interest. The study sponsor had no involvement in study design, data collection, analysis, or interpretation, writing of the paper, or the decision to submit the paper for publication.

References

American Psychiatric Association. Practice guideline for the treatment of patients with bipolar disorder (revision). Am J Psychiatry 2002;159 (4 Suppl):1–50.

Ayuso-Gutierrez JL, Ramos-Brieva JA. The course of manic-depressive illness. A comparative study of bipolar I and bipolar II patients. J Affect Disord 1982;4:9–14.

Berk M, Dodd S. Bipolar II disorder: a review. Bipolar Disord 2005;7:11–21.

Del Zompo M, Ardau R, Palmas MA, Bocchetta A, Reina A, Piccardi MP. Lithium response: association study with two candidate genes. Mol Psychiatry 1999;4:S66–7.

Diekmann D, Brill S, Garrett MD, Totty N, Hsuan J, Monfries C, et al. Bcr encodes a GTPase-activating protein for p21rac. Nature 1991;351:400–2.

Eagan MF, Kojima M, Callicott JH, Goldberg TE, Kolachana BS, Bertolino A, et al. The BDNF val66met polymorphism affects activity-dependent secretion of BDNF and human memory and hippocampal function. Cell 2003;112:257–69.

Fioretos T, Voncken JW, Baram TZ, Kamme F, Groffen J, Heisterkamp N. Regional localization and developmental expression of the BCR gene in rodent brain. Cell Mol Biol Res 1995;41:97–102.

Gasperini M, Scherillo P, Manfredonia MG, Franchini L, Smeraldi E. A study of relapses in subjects with mood disorder on lithium treatment. Eur Neuropsychopharmacol 1993;3:103–10.

Gelenberg AJ, Pies R. Matching the bipolar patient and the mood stabilizer. Ann Clin Psychiatry 2003;15:203–16.

Grof P, Duffy A, Cavazzoni P, Grof E, Garnham J, MacDougall M, et al. Is response to prophylactic lithium a familial trait? J Clin Psychiatry 2002;63: 942–7.

Harwood AJ. Lithium and bipolar mood disorder: the inositol-depletion hypothesis revisited. Mol Psychiatry 2005;10:117–26.

Hashimoto R, Okada T, Kato T, Kosuga A, Tatsumi M, Kamijima K, et al. The breakpoint cluster region gene on chromosome 22q11 is associated with bipolar disorder. Biol Psychiatry 2005;57:1097–102.

Ikeda A, Kato T. Biological predictors of lithium response in bipolar disorder. Psychiatry Clin Neurosci 2003;57:243–50.

Kleindienst N, Engel R, Greil W. Which clinical factors predict response to prophylactic lithium? A systematic review for bipolar disorders. Bipolar Disord 2005;7:404–17.

Lemmon MA, Ferguson KM, Abrams CS. Pleckstrin homology domains and the cytoskeleton. FEBS Lett 2002;513:71–6.

Mamdani F, Sequeira A, Alda M, Grof P, Rouleau G, Turecki G. No association between the PREP gene and lithium responsive bipolar disorder. BMC Psychiatry 2007;26:7–9.

Masui T, Hashimoto R, Kusumi I, Suzuki K, Tanaka T, Nakagawa S, et al. Lithium response and Val66Met polymorphism of the brain-derived neurotrophic factor gene in Japanese patients with bipolar disorder. Psychiatr Genet 2006;16:49–50.

Michelon L, Meira-Lima I, Cordeiro Q, Miguita K, Breen G, Collier D, et al. Association study of the INPP1, 5HTT, BDNF, AP-2beta and GSK-3beta GENE variants and restrospectively scored response to lithium prophylaxis in bipolar disorder. Neurosci Lett 2006;403:288–93.

Negishi M, Katoh H. Rho family GTPases as key regulators for neuronal network formation. J Biochem (Tokyo) 2002;132:157–66.

Rybakowski JK, Suwalska A, Skibinska M, Szczepankiewicz A, Leszczynska-Rodziewicz A, Permoda A, et al. Prophylactic lithium response and polymorphism of the brain-derived neurotrophic factor gene. Pharmacopsychiatry 2005;38:166–70.

Serretti A, Lilli R, Mandelli L, Lorenzi C, Smeraldi E. Serotonin transporter gene associated with lithium prophylaxis in mood disorders. Pharmacogenomics J 2001;1:71–7.

Serretti A, Lorenzi C, Lilli R, Mandelli L, Pirovano A, Smeraldi E. Pharmacogenetics of lithium prophylaxis in mood disorders: analysis of COMT, MAO-A, and Gbeta3 variants. Am J Med Genet 2002;114:370–9.

Smoller JW, Finn CT. Family, twin, and adoption studies of bipolar disorder. Am J Med Genet C 2003;123:48–58.

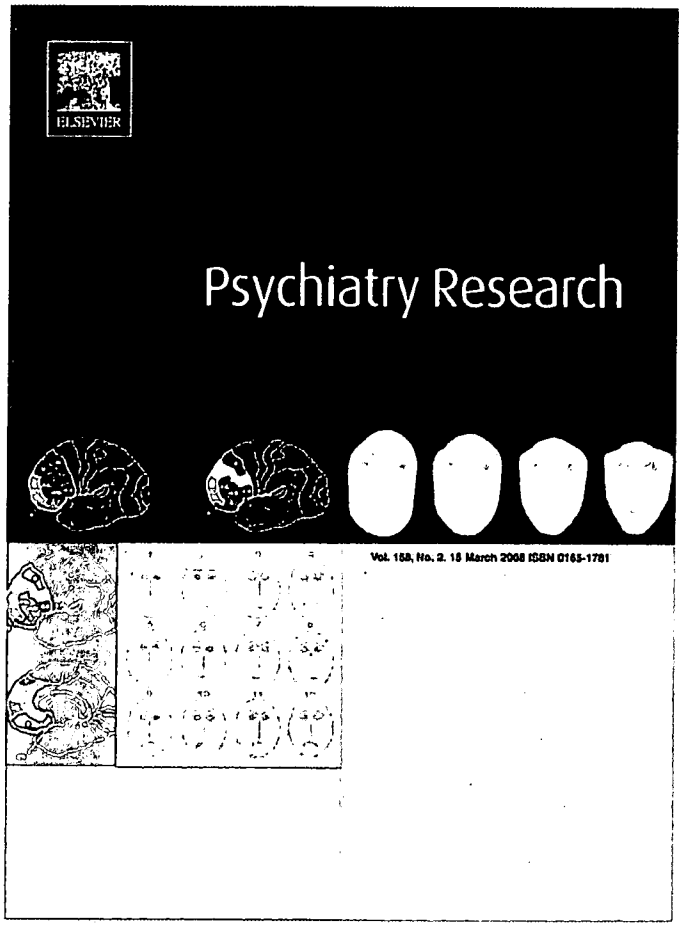

Available online at www.sciencedirect.com
ScienceDirect
Psychiatry Research 158 (2008) 251–255
PSYCHIATRY RESEARCH
www.elsevier.com/locate/psychres

Brief report

IQ decline and memory impairment in Japanese patients with chronic schizophrenia

Hiroaki Hori [a,b,*], Hiroko Noguchi [a], Ryota Hashimoto [a,c], Shigeo Okabe [b], Osamu Saitoh [d], Hiroshi Kunugi [a]

[a] *Department of Mental Disorder Research, National Institute of Neuroscience, National Center of Neurology and Psychiatry, 4-1-1, Ogawahigashi, Kodaira, Tokyo, 187-8502, Japan*
[b] *Department of Cell Biology, School of Medicine, Tokyo Medical and Dental University, 1-5-45, Yushima, Bunkyo-ku, Tokyo, 113-8519, Japan*
[c] *Osaka-Hamamatsu Joint Research Center for Child Mental Development, Osaka University Graduate School of Medicine, D3, 2-2, Yamadaoka, Suita, Osaka, 565-0871, Japan*
[d] *Department of Psychiatry, Musashi Hospital, 4-1-1, Ogawahigashi, Kodaira, Tokyo, 187-0031, Japan*

Received 24 August 2007; received in revised form 29 October 2007; accepted 1 November 2007

Abstract

The extent of IQ decline due to the development of illness in patients with chronic schizophrenia and the degree of memory impairment relative to such IQ decline still remain unclear. Our results suggest that schizophrenia patients experience marked IQ decline due to the development of illness and their wide-ranging memory impairments are even more severe than the IQ decline.

Keywords: Schizophrenia; IQ; Memory

1. Introduction

Cognitive impairment is a core feature of schizophrenia, with a great impact on patients' daily lives. Those therapies that have the potential to improve cognitive deficits of patients with schizophrenia, including cognitive remediation therapy (Medalia et al., 1998; Wykes et al., 2003), as well as the favorable effects of atypical antipsychotic drugs on cognition (Bilder et al., 2002; Harvey et al., 2006; Keefe et al., 2006), have been attracting increasing attention from researchers and clinicians. From this viewpoint, the precise delineation of cognitive impairments in schizophrenia patients is essential.

Intellectual deficits in patients with chronic schizophrenia have been reliably identified (Heinrichs and Zakzanis, 1998; Dickinson et al., 2004) with some ongoing debate as to "whether it is possible to be schizophrenic yet neuropsychologically normal" (Palmer et al., 1997; Kremen et al., 2000; Wilk et al., 2005); however, the extent of IQ decline caused by the development of schizophrenia remains unclear because the premorbid IQ scores of persons who later develop schizophrenia are lower than

* Corresponding author. Department of Mental Disorder Research, National Institute of Neuroscience, National Center of Neurology and Psychiatry, 4-1-1, Ogawahigashi, Kodaira, Tokyo, 187-8502, Japan. Tel.: +81 42 341 2711; fax: +81 42 346 1744.
E-mail address: balius26@hotmail.com (H. Hori).

0165-1781/$ - see front matter © 2007 Elsevier Ireland Ltd. All rights reserved.
doi:10.1016/j.psychres.2007.11.002

those of their peers (Fuller et al., 2002; Reichenberg et al., 2005). Impairments in memory, working memory, and attention in patients with schizophrenia are well documented (Aleman et al., 1999; Silver et al., 2003; Hori et al., 2006), but the relationship of these cognitive deficits to the possible decline in IQ has not been established. Here we assessed cognitive functions including intellectual and wide-ranging memory functioning in patients with chronic schizophrenia in relation to age- and premorbid IQ-matched healthy controls.

2. Materials and methods

Eighty-two patients who met the DSM-IV criteria (American Psychiatric Association, 1994) for schizophrenia participated in this study. All patients were receiving antipsychotic drugs at the National Center of Neurology and Psychiatry (NCNP), Musashi Hospital and were clinically stable at the time of the neuropsychological tests. Eighty-two age- and premorbid IQ-matched healthy volunteers were recruited from hospital staff and their associates and also from the community. Healthy participants were interviewed by a research psychiatrist using the Japanese version of the Mini-International Neuropsychiatric Interview (MINI, Sheehan et al., 1998) to confirm the absence of any psychiatric illnesses. A portion of the subjects were from our previous sample (Hori et al., 2006). Written informed consent was obtained from all subjects prior to their inclusion in the study. The study was approved by the ethics committee of the NCNP.

Premorbid IQ was estimated with the Japanese Adult Reading Test (JART, Matsuoka et al., 2002; 2006), a Japanese version of the National Adult Reading Test (NART, Nelson and Wilson, 1991). This test is considered to provide an estimate of premorbid IQ in schizophrenia patients (Uetsuki et al., 2006), which is consistent with the original NART (Crawford et al., 1992; O'Carroll et al., 1992). In this test, subjects were required to read out 100 idioms of Han-Chinese characters (Japanese kanji characters). JART-estimated premorbid IQ was calculated for each subject according to previous reports (Matsuoka et al., 2002, 2006). The full version of the Wechsler Memory Scale-Revised (WMS-R, Wechsler, 1987; Sugishita, 2001) was administered to all participants. Outcome measures of the WMS-R were verbal memory, visual memory, delayed recall, auditory attention, visual attention, verbal working memory, and visual working memory. To precisely assess subjects' current intellectual function, a full version of the Wechsler Adult Intelligence Scale-Revised (WAIS-R, Wechsler, 1981; Shinagawa et al., 1990) was administered, yielding age-corrected indices of verbal, performance, and full-scale IQs.

Schizophrenic symptoms were assessed by an experienced research psychiatrist in 46 of the 82 patients using the Positive and Negative Syndrome Scale (PANSS, Kay et al., 1987). Daily doses of antipsychotics and anticholinergic antiparkinsonian drugs were converted to chlorpromazine equivalents (CPZeq) and biperiden equivalents (BPDeq), respectively, using published guidelines (American Psychiatric Association, 1997; Inagaki et al., 1999; Minzenberg et al., 2004).

Results are reported as mean±standard deviation (S.D.). Demographic characteristics and cognitive test results were compared between groups. We used *t*-test or analysis of variance (ANOVA) to compare mean scores and the χ^2 tests to compare categorical variables. Analysis of covariance (ANCOVA) was used to compare means between groups, controlling for confounding variables. Statistical significance was set at two-tailed $P<0.05$. Analyses were performed using the Statistical Package for the Social Sciences (SPSS) version 11.0 (SPSS Japan, Tokyo).

3. Results

Male/female ratios of patients and controls were 48/34 and 25/57, respectively, indicating that the patient group had a greater representation of males ($\chi^2(1)=13.06$, $P<0.001$). The mean ages of the patients and controls were 44.3±13.8 and 44.2±14.9, respectively ($t=0.05$, $df=162$, $P=0.96$). The mean years of education of the patients and controls were 13.4±2.5 and 14.1±2.2, respectively ($t=1.88$, $df=162$, $P=0.06$). The JART-predicted premorbid IQ scores of patients and controls were 102.2±11.6 and 102.3±7.4, respectively ($t=0.46$, $df=137.8$, $P=0.96$). Of the 82 patients, 56 were outpatients and 26 were inpatients. The mean age of illness onset was 24.7±8.8. Illness duration was 19.6±13.7 years, demonstrating that our patients were in the chronic phase of schizophrenia. CPZeq and BPDeq were 781.7±710.1 and 2.2±2.0, respectively. PANSS positive, negative, and total scores were 13.9±6.7, 19.1±7.1, and 62.1±17.9, respectively.

Verbal, performance, and full-scale IQs of patients with schizophrenia and healthy controls are presented in Supplementary Table 1. ANOVA showed that these three IQ indices in patients were significantly lower than those in controls (all $P<0.001$). The VIQ/PIQ ratios of patients and controls were 1.08±0.18 and 0.95±0.11, respectively ($F=22.5$, $df=1,160$, $P<0.001$, by ANCOVA with gender as a covariate). Scores of 13 subscales of the WMS-R in patients and controls are also shown in Supplementary Table 1. Patients performed significantly

more poorly than controls on all these cognitive domains (all $P<0.001$), except for auditory attention ($P=0.15$). Fig. 1(a) shows mean scores of the patients and controls on JART-estimated IQ, WAIS-R full-scale IQ, and the main three memory indices of the WMS-R. Dips of current IQ and all memory domains in patients are apparent, although the two groups are matched for the JART-estimated premorbid IQ.

To control for the current IQ and gender effects on these test results, ANCOVA was used with full-scale IQ and gender as covariates. It revealed that patients performed significantly more poorly than controls on verbal memory, visual memory, delayed recall, visual attention, and verbal working memory, even after controlling for full-scale IQ and gender (Supplementary Table 1). To confirm these results, additional comparisons were made between patients whose current IQ scores were within normal limit (IQ-WNL patients, defined as WAIS-R full-scale IQ ≥ equal to or greater than 85; $n=46$) and total controls ($n=82$). Fig. 1(b) summarizes the results, showing that there was no difference in current IQ between IQ-WNL patients (mean IQ: 98.85±8.55) and controls (mean IQ: 101.95±11.30), while these patients still showed significantly lower scores on all three memory indices compared with controls. On the other hand, the JART-estimated premorbid IQ of IQ-WNL patients was significantly higher than that of controls.

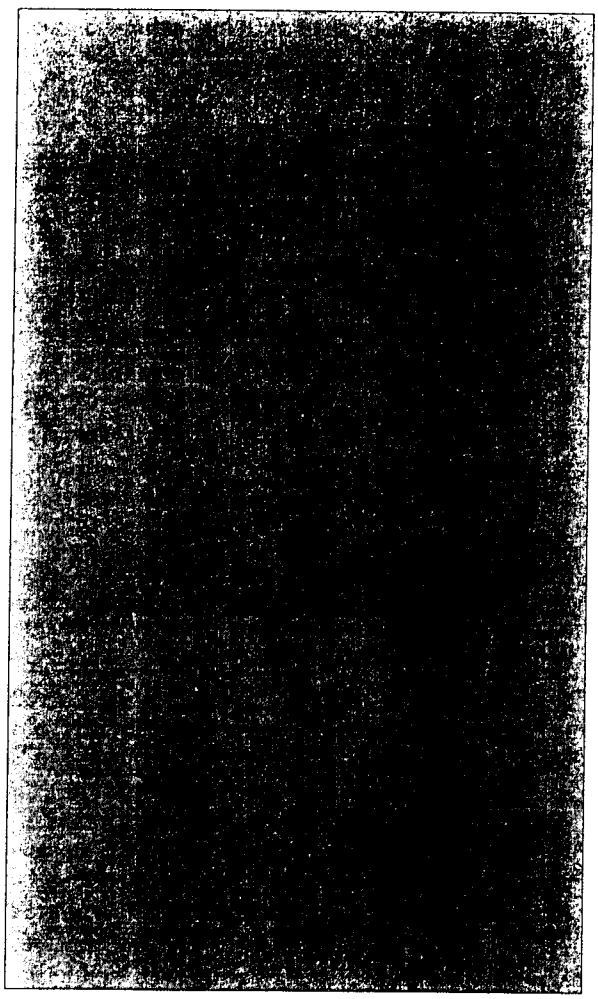

Fig. 1. Mean scores of patients and controls on JART IQ, WAIS-R full-scale IQ, Verbal memory, Visual memory, and Delayed recall indices (WMS-R). (a) total patients ($n=82$) vs. total controls ($n=82$) and (b) IQ-WNL patients (defined as WAIS-R full-scale IQ ≥ 85, $n=46$) vs. total controls ($n=82$).***$P<0.001$.

4. Discussion

In the present study we examined intellectual and memory functions in patients with chronic schizophrenia relative to age- and premorbid IQ-matched healthy controls. Our results confirmed that patients with chronic schizophrenia have wide-ranging cognitive impairments, consistent with the literature on schizophrenia.

The relationship of the development of schizophrenia to declining IQ scores has been confounded by findings that premorbid intelligence itself is likely to be lower in persons who later develop schizophrenia than in their peers (Fuller et al., 2002; Reichenberg et al., 2005). To address this issue, we employed a premorbid IQ-matched case-control sample. Although the cross-sectional nature of the present study does not allow any definite conclusions to be drawn concerning the time when the IQ decline actually occurred (i.e., during the prodromal stage, immediately after illness onset, or during the chronic course of illness), the observed differences in current IQs between patients and controls provide evidence for marked IQ decline due to the development of schizophrenia. Means of estimated premorbid IQ and current full-scale IQ in patients were 102.20 and 87.68, respectively, suggesting an approximate 1 S.D. decline in IQ score related to the development of illness. On the other hand, the subgroup of patients whose current IQ was within normal limits (and thus similar to that of controls) showed significantly higher premorbid IQ as estimated by the JART than controls (Fig. 1(b)), which favors the view that even neuropsychologically normal patients with chronic schizophrenia have compromised cognitive functioning relative to their presumed premorbid level of intellectual function (Kremen et al., 2000). Furthermore, in the present study performance IQ of the patients was more severely impaired than verbal IQ, congruent with prior reports (Heinrichs and Zakzanis, 1998).

Pervasive memory impairment in patients with schizophrenia relative to premorbid IQ-matched controls was